Accepted Manuscript

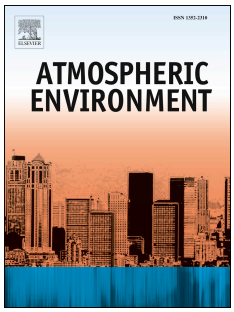

Characterization of atmospheric black carbon and co-pollutants in urban and rural areas of Spain

M. Becerril-Valle, E. Coz, A.S.H. Prévôt, G. Močnik, S.N. Pandis, A.M. Sánchez de la Campa, A. Alastuey, E. Díaz, R.M. Pérez, B. Artíñano

PII: S1352-2310(17)30605-2

DOI: 10.1016/j.atmosenv.2017.09.014

Reference: AEA 15552

To appear in: *Atmospheric Environment*

Received Date: 26 July 2017

Revised Date: 5 September 2017

Accepted Date: 8 September 2017

Please cite this article as: Becerril-Valle, M., Coz, E., Prévôt, A.S.H., Močnik, G., Pandis, S.N., Sánchez de la Campa, A.M., Alastuey, A., Díaz, E., Pérez, R.M., Artíñano, B., Characterization of atmospheric black carbon and co-pollutants in urban and rural areas of Spain, *Atmospheric Environment* (2017), doi: 10.1016/j.atmosenv.2017.09.014.

Characterization of atmospheric black carbon and co-pollutants in urban and rural areas of Spain

M. Becerril-Valle[1], E. Coz[1], A. S. H. Prévôt[2], G. Močnik[3,4], S. N. Pandis[5,6,7], A. M. Sánchez de la Campa[8,9], A. Alastuey[10], E. Díaz[1], R. M. Pérez[11], B. Artíñano[1]

[1]CIEMAT, "Atmospheric Pollution 1", Associated Unit to CSIC, Department of Environment, CIEMAT, Madrid, ES-28040, Spain

[2]Laboratory of Atmospheric Chemistry, Paul Scherrer Institute (PSI), Villigen-PSI, CH- 5232, Switzerland

[3]Aerosol d.o.o., Ljubljana, SI-1000, Slovenia

[4]Condensed Matter Physics Department, Jožef Stefan Institute, SI-1000 Ljubljana, Slovenia

[5]Institute of Chemical Engineering Sciences, ICE-HT. Patras, GR-26504, Greece

[6]Department of Chemical Engineering, University of Patras, Patras, GR-26504, Greece

[7]Department of Chemical Engineering, Carnegie Mellon University, Pittsburgh, PA-15213, USA

[8]Associated Unit CSIC-University of Huelva "Atmospheric Pollution", Centre for Research in Sustainable Chemistry (CIQSO), University of Huelva, Huelva, ES-21071, Spain

[9]Department of Geology, Faculty of Experimental Sciences, University of Huelva, Huelva, ES-21071, Spain

[10]Institute of Environmental Assessment and Water Research (IDAEA-CSIC), Barcelona, ES-08034, Spain

[11]Department of Technology, CIEMAT, Madrid, ES-28040, Spain

Correspondence to: M. Becerril-Valle (marta.becerril@ciemat.es)

ABSTRACT

A one-year black carbon (BC) experimental study was performed at three different locations (urban traffic, urban background, rural) in Spain with different equivalent BC (eBC) source characteristics by means of multi-wavelength Aethalometers. The Aethalometer model was used for the source apportionment study, based on the difference in absorption spectral dependence of emissions from biomass burning (bb) and fossil fuel (ff) combustion. Most studies use a single bb and ff absorption Ångström exponent (AAE) pair (AAE_{bb} and AAE_{ff}), however in this work we use a range of AAE values associated with fossil fuel and biomass burning based on the available measurements, which represents more properly all conditions. A sensitivity analysis of the source specific AAE was carried out to determine the most appropriate AAE values, being site dependent and seasonally variable. Here we present a methodology for the determination of the ranges of AAE_{bb} and AAE_{ff} by evaluating the correlations between the source apportionment of eBC using the Aethalometer model with four biomass burning tracers measured at the rural site. The best combination was AAE_{bb} = [1.63 – 1.74] and AAE_{ff} = [0.97 – 1.12]. Mean eBC values (±SD) obtained during the period of study were 3.70 ± 3.73 $\mu g \cdot m^{-3}$ at the traffic urban site, 2.33 ± 2.96 $\mu g \cdot m^{-3}$ at the urban background location, and 2.61 ± 5.04 $\mu g \cdot m^{-3}$ in the rural area. High contributions of eBC to the PM_{10} mass were found (values up to 21 % in winter), but with high eBC/PM_{10} variability. The hourly mean eBC_{ff} and eBC_{bb} concentrations varied from 0 to 51 $\mu g \cdot m^{-3}$ and from 0 to 50 $\mu g \cdot m^{-3}$ at the three sites, respectively, exhibiting distinct seasonal and daily patterns. The fossil fuel combustion was the dominant eBC source at the urban sites, while biomass burning dominated during the cold season (88 % of eBC_{bb}) in the rural area. Daily $PM_{2.5}$ and PM_{10} samples were collected using high-volume air samplers and analyzed for OC and EC. Analysis of biomass burning tracers and organic (OC) and elemental (EC) carbon in the rural area indicate that biomass combustion is the main source, while OC and EC indicate a lower influence of this source at the urban site.

Keywords: carbonaceous aerosols; black carbon; absorption Ångström exponent; source apportionment; fossil fuel; biomass burning.

1. INTRODUCTION

Atmospheric aerosols influence the Earth's energy balance both directly, through absorption and scattering of solar radiation in the atmosphere (Shine and Foster, 1999; Haywood and Boucher, 2000; Satheesh and Krishnamoorthy, 2005; IPCC, 2007), and indirectly, by acting as cloud condensation nuclei or ice nuclei (Twomey, 1974; Albrecht, 1989; Lohmann and Feichter, 2005; IPCC, 2013). Some aerosol components (i.e. black carbon) may have a net warming impact, while others (i.e. nitrates, sulfates, organic carbon, etc.) may have a cooling effect (Chýlek and Coakley, 1974; IPCC, 2013). At the same time, aerosols reduce visibility, have an important impact on air quality, and also adversely affect human health (Dockery et al., 1993; Horvath, 1995; Beeson et al., 1998; Harrison and Yin, 2000; Pope III, 2002; Wang and Christopher, 2003; Pope and Dockery, 2006).

The use of terms such as soot, BC, black smoke (BS), EC, light-absorbing aerosols, etc., has caused a great deal of confusion within the air quality monitoring and aerosol research communities. To avoid this, the Global Atmospheric Watch (GAW) Scientific Advisory Group (GAW/WMO, 2012; Petzold et al., 2013) recommended that when BC is measured using optical techniques, the term equivalent black carbon (eBC) should be used instead of BC to stress that the determined optical signal gives an equivalent mass concentration to the measured absorption.

Even if the chemical composition of aerosols is characterized by large spatial and temporal variability (Moorthy et al., 2009; Mohr et al., 2011; Piazzola et al., 2012; Abdeen et al., 2014), carbonaceous aerosols typically comprise more than half of the submicron fraction of atmospheric particulate matter (PM) (Gelencsér, 2004; Putaud et al., 2004; Putaud et al., 2010; Zhu et al., 2014). The major components of carbonaceous particulate matter in the atmosphere are organic carbon (OC) and a refractory (and also highly light absorbing) fraction resistant to oxidation at temperatures below 400 ºC, known as elemental carbon (EC) (Penner and Novakov, 1996). When the elemental carbon is measured using optical methods relying on its strongly light absorbing character, it is called black carbon (BC). The carbonate or mineral carbon (CC) is usually a minor contributor to the total carbonaceous aerosol (Seinfeld and Pankow, 2003). OC can be directly emitted from sources as primary organic aerosol (POA) or can be produced by atmospheric reactions involving gaseous organic precursors forming secondary organic aerosol (SOA) (Seinfeld and Pandis, 2006). Although EC and BC have been often used indistinctly in the literature, refer to a similar fraction of the carbonaceous aerosol and are supposed to be

comparable, they can have different thermal, optical, and chemical behavior and are distinguished by the measurement technique and protocol used.

BC is emitted during the incomplete combustion of fossil fuels, biofuels, and biomass burning and absorbs at all wavelengths of solar radiation (IPCC, 2013). It is always co-emitted with other organic compounds and inorganic gases, such as nitrogen oxides (NO_x) and sulfur dioxide (SO_2) (US EPA, 2012; Bond et al., 2013). BC is refractory (stability at very high temperatures, with a vaporization temperature near 4000 K); insoluble in water and common organic solvents, and it exists in nature as an aggregate of small carbon spherules. These physical properties make it unique and distinguishable from other forms of carbon and carbon compounds contained in atmospheric aerosols (Bond et al., 2013; Petzold et al., 2013). BC, together with methane (CH_4) and tropospheric ozone (O_3), is one of the most important contributor to current global warming after carbon dioxide (CO_2) (UNEP-CCAC, 2014). UNEP and WMO (2011) have estimated that implementation of proposed BC and CH_4 control measures by 2030 could prevent up to 0.5°C of additional warming by 2050.

Additionally, the review of the results of all available toxicological studies suggested that BC (measured as EC) may not be a major directly toxic component of fine PM, but it may operate as a universal carrier of a wide variety of, especially, combustion-derived chemical constituents of varying toxicity to sensitive targets in the human body such as the lungs, the body's major defense cells and possibly the systemic blood circulation (WHO, 2012). BC and co-pollutants make up for the majority of the fine particulate matter ($PM_{2.5}$), currently considered a major environmental cause of respiratory and cardiovascular diseases, with a global estimation of more than 6 million premature deaths annually from exposure to indoor and outdoor (Lim et al., 2012).

There are several available light-absorption based eBC measurement methods: (a) filter transmission measurements using instruments such as the Aethalometer (Hansen et al., 1984; Drinovec et al., 2015), the Particle Soot Absorption Photometer (PSAP; Bond et al., 1999), the Multi-Angle Absorption Photometer (MAAP; Petzold and Schönlinner, 2004) and the Continuous Soot Monitoring System (COSMOS; Miyazaki et al., 2008); (b) photo-acoustic techniques: the absorption of the air suspended aerosol through the pressure fluctuation due to absorption can be measured for example by the Photo-Acoustic Soot Spectrometer (PASS) (Arnott et al., 1999); and (c) photo-thermal interferometry techniques (folded-Jamin interferometer; Jamin, 1856).

Sandradewi et al., (2008a; b) suggested that the absorption Ångström exponent (AAE), characterizing the spectral dependence of aerosol light absorption (Kirchstetter et al., 2004; Moosmüller et al., 2011; Bond et al., 2013), can be used to quantify the contribution of fossil fuel and biomass burning to the total eBC mass concentration. For this purpose, they developed the so-called "Aethalometer model", a two-component method to apportion eBC to fossil fuel (eBC_{ff}) and to biomass burning (eBC_{bb}), which has been used extensively in the last recent years (Favez et al., 2009; Martinsson et al., 2017; Titos et al., 2017; Zotter et al., 2017).

As in other regions in Europe (Putaud et al., 2010) previous studies in Spain (Querol et al., 2004b) confirmed that carbonaceous aerosol was one of the main components of the aerosol in urban and rural areas. Source apportionment studies in Madrid, pointed to traffic emissions as the dominant source of carbonaceous aerosol (Plaza et al., 2011; Salvador et al., 2004, 2012) leading in many occasions to PM limit value exceedances.

PM_{10} limit values are also exceeded in other urban and rural areas of Spain (Querol et al., 2004a). One of these latter is the Andalusian olive groves region of Jaén, which in the last years has experienced both PM_{10} daily limit value and $PM_{2.5}$ annual limit value exceedances (Junta de Andalucía, 2015). High concentration levels are recorded during the autumn and winter months, and have been associated in principle to the increase of domestic biomass burning in these periods of the year (Salvador et al., 2016).

The quantification of atmospheric eBC and co-pollutants mass concentrations, as well as the identification and characterization of its sources, are of particular interest for designing efficient mitigation strategies.

The main purpose of this work is to characterize the atmospheric black carbon and the co-pollutants in different areas. To this end, we conduct a source apportionment study of eBC with rather different characteristics in terms of eBC sources. We present an evaluation of the Aethalometer model by comparing its outputs to the specific inorganic (potassium associated with biomass burning) and organic compounds (three monosaccharide anhydrides: levoglugosan, mannosan, and galactosan) used as biomass burning tracers to select the best option of the absorption Ångström exponent for biomass burning. In addition, we evaluate the elemental and organic carbon and their relationship with eBC. This type of research has not been previously carried out in the selected areas, even though they are characterized by high particulate matter levels.

2. METHODOLOGY

2.1 Measurement Sites

Simultaneous measurements were carried out during a one-year period at three sites in Spain (Fig. 1). Two of them are urban sites located in Madrid: one at the Research Centre for Energy, Environment, and Technology (CIEMAT) facilities, an urban background area; and the second at Escuelas Aguirre, a traffic urban site. A third site (Villanueva) was located in a rural area of Andalusia (Villanueva del Arzobispo, Jaén).

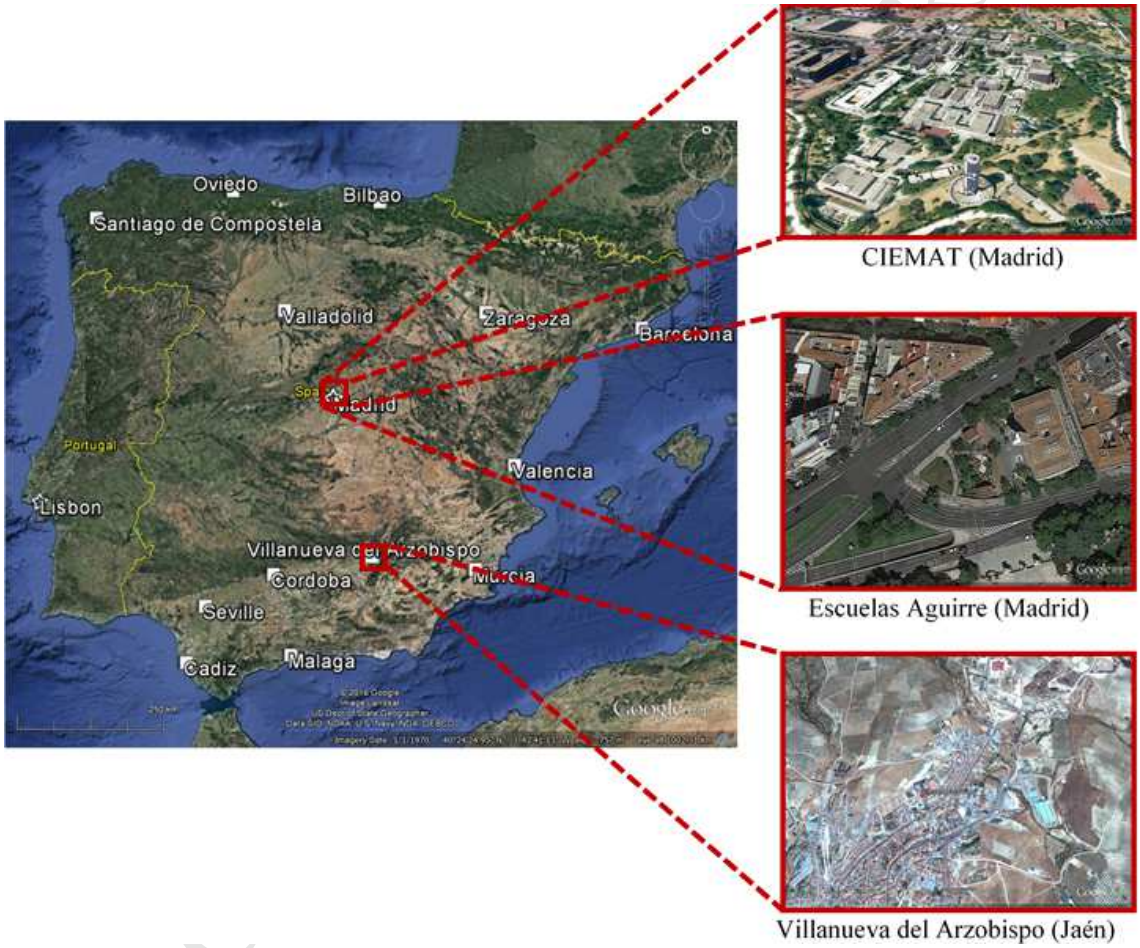

Figure 1. Measurement sites used in this study (source: Google Earth).

Madrid sites

Madrid is the most populous city in Spain with more than 3 million inhabitants in the urban core. In contrast to a great number of the other large European cities, there is very low heavy industrial activity in the metropolitan area. Traffic and commercial and domestic heating are the major local sources of air pollution (Madrid City Council, 2015) leading to significant air pollution episodes during the autumn and

157 winter periods under atmospheric anticyclonic stagnation conditions (Artíñano et al., 2003; Plaza et al.,
158 2011). Madrid's climate is considered as Mediterranean continental (Köppen climate classification) with
159 dry and hot summers and cold winters. Even though levels of air pollution seem to have experienced a
160 significant decrease in recent years (Salvador et al., 2015), mean ambient concentrations of all primary
161 pollutants increased during 2015 compared to previous years with the exception of ozone, which
162 remained stable, according to the latest report on air quality published by the Madrid City Council
163 (Madrid City Council, 2016). This increase could be associated with adverse meteorological conditions,
164 such as intense winter atmospheric pollution episodes which took place during that year.

165 One of the urban sites of this study, CIEMAT (40°27′23″N 3°43′32″W, 669 m ASL), is located
166 in the NW part of the city, in a non-residential area at the edge of the main University Campus (Ciudad
167 Universitaria). This site can be considered as representative of the urban background according to the
168 European Environment Agency (EEA, 1999) criteria for air quality monitoring stations classification.

169 The other urban site, Escuelas Aguirre (40°25′17.63″N 3°40′56.35″W, 672 m ASL), is located in
170 one of the stations of the Madrid City Council air quality monitoring network. This is a traffic urban site,
171 located in the city center at the intersection of two major avenues close to El Retiro Park. The surrounding
172 area is characterized by intense road traffic leading to high pollution levels (both NOx and PM_{10})
173 measured at this station.

174

175 *Villanueva del Arzobispo, Jaén*

176 The rural site (Villanueva) is located in the region of Jaén, Andalusia, the largest area of olive
177 groves of Spain. In recent years, olive waste is being used in the area for power generation, which could
178 contribute to air quality problems in this region (Sigsgaard et al., 2015). At the same time, the economic
179 crisis has resulted in an increasing use of biomass (wood and olive pits) for domestic heating during the
180 cold months adding another air pollution source in this area. The measurement site forms part of the Air
181 Quality Monitoring Network of Regional Government of Andalusia (Junta de Andalucía) placed in
182 Villanueva del Arzobispo (38º10′27.80″N 3º0′18.30″W, 620 m ASL), a small town with about 8700
183 inhabitants. This station has exceeded the European PM_{10} daily limit value during the last 5 years, mainly
184 during the autumn and winter months, and the $PM_{2.5}$ annual limit value in 2016 (the unique station in
185 Spain exceeding this limit value) (Junta de Andalucía, 2016; MAPAMA, 2017). This geographical area

has a continental climate characterized by long periods of atmospheric stability and frequent fog episodes in winter and dry and very warm summers.

2.2 Measurements and instrumentation

2.2.1. Meteorological variables

Meteorological information was obtained at CIEMAT from a fully equipped meteorological tower that measures wind direction and speed at 52 m AGL, precipitation, and solar radiation at 31 m AGL, atmospheric temperature and relative humidity at 4 m AGL, and pressure at ground level. Data are recorded every 10 minutes. In the case of Escuelas Aguirre, the meteorological information was provided by the State Meteorological Agency of Spain (AEMET) from the standard station located in El Retiro park. Wind direction and speed, precipitation, atmospheric temperature, relative humidity, and pressure are measured every 10 minutes. Meteorological information in Villanueva was provided by the Regional Government of Andalusia (Junta de Andalucía). Wind direction and speed, precipitation, atmospheric temperature, and relative humidity are measured at 4 m AGL in this station every 10 minutes.

In this work, data from the period December 22, 2014 to December 21, 2015 were analyzed. Astronomical seasons were considered to study the seasonal variation and Coordinated Universal Time (UTC) was used.

2.2.2. PM mass concentrations

Hourly average PM_{10} mass concentrations were obtained at CIEMAT from an optical particle counter monitor (Model GRIMM 1107, GRIMM Technologies, Inc.). In Escuelas Aguirre PM_{10} concentrations were provided by a Tapered Element Oscillating Microbalance (Model 1405-DF TEOM™, Thermo Scientific™). Finally, in Villanueva, PM_{10} concentrations were obtained with a Beta Continuous Ambient Particulate Monitor (Eberline FH62 I-R, Thermo Eberline). PM measurements of the three instruments were normalized against gravimetric methods through the gravimetric measurements of filter samples collected simultaneously with the aforementioned real-time PM instruments.

2.2.3. Ambient filter sampling and chemical analyses

$PM_{2.5}$ and PM_{10} filter samples were collected at CIEMAT and in Villanueva, whereas sample filters measurements at Escuelas Aguirre were not available. Ambient aerosol samples were collected on quartz-fiber filters for 24-h using high-volume (30 $m^3 \cdot h^{-1}$). $PM_{2.5}$ and PM_{10} samplers (model MCV CAV-A/M) were used with DIGITEL inlets (model DHA-80). Filters were weighed before and after sampling in order to determine the PM mass concentration by the gravimetric method following standard procedures (UNE-EN 12341:1999; UNE-EN 14907:2006).

21 filter samples in each fraction (PM_{10} and $PM_{2.5}$) were collected from November 2014 to September 2015 at CIEMAT and 59 filter samples in each fraction (PM_{10} and $PM_{2.5}$) from November 2014 to June 2015 at Villanueva. Tables S1 and S2 summarize the sampling dates, size fractions and samples collected at each site.

OC and EC concentrations were determined by a Thermal-Optical Transmittance (TOT) method (Pio et al., 1994; Birch and Cary, 1996; Sánchez de la Campa et al., 2009), adapted from Huntzicker et al., (1982) using a Sunset Laboratory OCEC Analyzer and the EUSAAR2 temperature protocol (Cavalli et al., 2010).

Levoglucosan, mannosan and galactosan concentrations were quantified using the analytical method described by Alier et al. (2013). Filters were ultrasonically extracted with dichlomoethane:methanol (2:1) by triplicate. Sedoheptulosan was used as surrogate standard. An aliquot of concentrated extract was derivatized with BSTFA/TMCS (99:1), using pyridine as catalyst and palmitic acid-D31 as internal standard, maintaining the mixture in an oven at 70 ºC for one hour. Trimethylsilyl derivatives of anhydrosugars were analyzed by GC/MS. These compounds are derivatives of glucose, mannose, and galactose respectively and are used as tracers for biomass burning (Simoneit et al., 1999; Simoneit, 2002; Alves, 2008; Krumal et al., 2012; Cong et al., 2015), as they are major components of biomass burning organic aerosol (Simoneit et al., 1999; Graham et al., 2002). Levoglucosan is produced during the pyrolysis of cellulose (Nolte et al., 2001; Simoneit, 2002; Krumal et al., 2012), while its isomers mannosan and galactosan are produced from hemicellulose (Nolte et al., 2001).

Some studies have found that water-soluble potassium (K^+) can be used as a tracer for biomass burning sources (Andreae, 1983; Echalar et al., 1995; Andreae et al., 1998). Total potassium (K) is emitted from biomass burning and as a component of dust emissions (Pio et al., 2008; Viana et al., 2008). In this study, total potassium was analyzed by Inductively Coupled Plasma Atomic Emission

Spectrometry (ICP-AES), therefore the biomass burning contribution (K_{bb}) has been estimated by subtracting the potassium of mineral origin obtained indirectly from aluminum oxide from this total potassium (Moreno et al., 2006; Alastuey et al., 2016).

2.2.4. eBC mass concentrations

Equivalent black carbon (eBC) mass concentrations were measured using three multi-wavelength Aethalometers (Magee Scientific Aethalometer model AE33, Aerosol d.o.o, Slovenia), with 10 μm inlets (BGI, MiniPM® Inlet) at a flow rate of 5 $Lmin^{-1}$. The new Aethalometer Model AE33 compensates for the "spot loading effect" in real-time (Drinovec et al., 2015). Data were recorded with 1-minute time resolution. Light attenuation by the aerosol particles deposited on a Teflon-coated glass fiber filter tape was measured at 7 wavelengths (λ = 370, 470, 520, 590, 660, 880, and 950 nm). The equivalent black carbon (eBC) mass concentration was calculated using the measurement at 950 nm wavelength with a mass absorption cross-section (MAC) of 7.19 $m^2 \cdot g^{-1}$ (Drinovec et al., 2015). The Ultraviolet-absorbing PM mass concentration was estimated at 470 nm, with a MAC of 14.54 $m^2 \cdot g^{-1}$ (Drinovec et al., 2015), which assumes the presence of organic compounds.

The Aethalometer used at CIEMAT is part of the ACTRIS European Infrastructure Network (http://www.actris.eu/) and regularly participates in the ACTRIS intercomparison exercises (February 2013 and September 2017). The Escuelas Aguirre instrument belongs to the Madrid City Council Air Quality Network and is subject to its maintenance and Quality Control procedures. The Villanueva instrument is owned by CIEMAT and is intercompared against the one operating at the CIEMAT station every year. The slope and its standard error of the linear least square regression through the origin of these two instruments was 0.96 ± 0.005 at 470 nm and at 950 nm, with a correlation coefficient (R^2) of 0.99 for both wavelengths.

2.3 The Aethalometer model

Due to the difference in the spectral dependence in absorption between biomass burning (bb) and fossil fuel (ff) emissions, it is possible to apportion equivalent black carbon to these two sources of aerosol by means of the Aethalometer model (Sandradewi et al., 2008b). Assuming that only these two sources contribute to absorption, the total absorption coefficient $b_{abs,total}(\lambda)$ at wavelength λ is equal to:

$$b_{abs,total}(\lambda) = b_{abs,ff}(\lambda) + b_{abs,bb}(\lambda) \quad (3)$$

where $b_{abs,ff}(\lambda)$ and $b_{abs,bb}(\lambda)$ are the absorption coefficients apportioned to fossil fuel combustion and biomass burning, respectively.

The relationship between aerosol composition and the wavelength dependence of the aerosol absorption light coefficient b_{abs} can be obtained by the power law fit (Ångström, 1929):

$$b_{abs} \propto \lambda^{-AAE} \quad (4)$$

where λ is the wavelength and AAE is the source specific absorption Ångström exponent (Sandradewi et al., 2008a). As in Sandradewi et al., (2008b), AAE has been estimated using the absorption coefficients of a pair of wavelengths (λ_1, λ_2) according to the Ångström relationship (Ångström, 1929):

$$AAE(\lambda_1, \lambda_2) = -\frac{\ln(b_{abs}(\lambda_1)/b_{abs}(\lambda_2))}{\ln(\lambda_1/\lambda_2)} \quad (5)$$

where $b_{abs}(\lambda_1)$ and $b_{abs}(\lambda_2)$ are the absorption coefficients at λ_1 and λ_2, respectively.

The source apportionment of eBC from biomass burning (eBC_{bb}) and fossil fuel (eBC_{ff}) may be derived from the following equations:

$$\frac{b_{abs,ff}(\lambda_1)}{b_{abs,ff}(\lambda_2)} = \left(\frac{\lambda_1}{\lambda_2}\right)^{-AAE_{ff}} \quad (6)$$

$$\frac{b_{abs,bb}(\lambda_1)}{b_{abs,bb}(\lambda_2)} = \left(\frac{\lambda_1}{\lambda_2}\right)^{-AAE_{bb}} \quad (7)$$

$$eBC_{ff} = \frac{b_{abs,ff}(\lambda_2)}{b_{abs,total}(\lambda_2)} \cdot eBC_{total}(\lambda_2) \quad (8)$$

$$eBC_{bb} = \frac{b_{abs,bb}(\lambda_2)}{b_{abs,total}(\lambda_2)} \cdot eBC_{total}(\lambda_2) \quad (9)$$

where AAE_{ff} and AAE_{bb} are the absorption Ångström exponents of fossil fuel and biomass burning of eBC, respectively.

In this work, light absorption measurements at λ_1 = 470 nm and λ_2 = 950 nm were used (Sandradewi et al., 2008b; Favez et al., 2010; Harrison et al., 2013) due to the fact that eBC from fossil fuel has a weak dependence on wavelength (i.e., AAE ~ 1), while eBC from biomass burning features stronger absorption spectral dependence and shows enhanced absorption at shorter wavelength (i.e., AAE > 1) (Kirchstetter et al., 2004; Russell et al., 2010). The absorption at 470 nm was used instead of the ultraviolet (UV) channel of the Aethalometer at 370 nm to minimize the interferences introduced by types of organic compounds, based on the sensitivity of the Aethalometer model due to different wavelength combinations carried out by Zotter et al., (2017), where it has been obtained that using the 370 nm wavelength resulted in larger residuals, a significant number of negative points and weaker correlations

with the fossil fraction of EC (EC_F/EC) derived from ^{14}C measurements. The estimated differences between the $AAE_{470-880}$ (calculated using the 470 and 880 nm measurements) and the $AAE_{470-950}$ (calculated using the 470 and 950 nm measurements) values were in the range of 4 to 8 % and the two measurements had a R^2 = 0.99 in all the three sites. Even though 880 nm is considered the standard channel for eBC measurement by Aethalometers, the 950 nm wavelength will be used in this work according to the results obtained in the sensitivity of the Aethalometer model using different pairs of wavelengths carried out by Zotter et al., (2017). Therefore, the rest of the analysis will be based on $AAE_{470-950}$.

Other studies (Herich et al., 2011; Fuller et al., 2014; Petit et al., 2015) have used other combinations of wavelengths (e.g. 370 nm and 880 nm, or 470 nm and 880 nm), often because of the constraints posed by the instrumentation used in their corresponding works. For example, the Magee Scientific Aethalometer models AE22 and AE42-2 measure light absorption only at 370 nm and 880 nm.

Selection of AAE_{ff} and AAE_{bb} values

Previous eBC source apportionment studies (Sandradewi et al., 2008a; Favez et al., 2010; Herich et al., 2011; Harrison et al., 2013; Petit et al., 2014) using the above Aethalometer model have assumed two single fixed AAE values for the estimation of the respective contributions of fossil fuel and biomass burning to ambient eBC concentrations. The main methodological novelty of this work is the use of a range of AAE values associated with fossil fuel (AAE_{ff}) and biomass burning (AAE_{bb}) based on the available measurements. These values of AAE were obtained with the following approach.

In the first step, a range of AAE values for fossil fuel (AAE_{ff}) and biomass burning (AAE_{bb}) was estimated. The representative values of AAE_{bb} were evaluated based on the correlations between the measured mass concentrations of the potassium associated with biomass burning (K_{bb}) and the three monosaccharide anhydrides (levoglugosan, mannosan, and galactosan) on one side, and eBC_{bb} mass concentrations obtained from the Aethalometer model on the other, in Villanueva. The contribution of biomass burning in that area is high in winter, mainly due to the use of wood stoves for domestic heating, as source apportionment studies have revealed (Salvador et al., 2016). The stability of the model output with respect to AAE_{ff} and AAE_{bb} was determined by monitoring the Pearson correlation coefficient for varying AAE_{ff} and AAE_{bb} in the range [0.80 - 1.20] and [1.60 - 2.50], respectively (Figs. S1 – S8). The AAE_{bb} values that maximize the R-Pearson coefficient were 1.63 between K_{bb} and eBC_{bb}, and 1.74

between the three organic compounds and eBC_{bb}. For these AAE_{bb} values, the variation of the R-Pearson coefficient was almost independent of AAE_{ff}. Thus, based on the goodness of the fit, the range of AAE_{bb} = [1.63 – 1.74] seems to be the optimal for our study. These values agree with the obtained in previous studies where radiocarbon (^{14}C) measurements of the fossil and non-fossil fractions of EC and OC were used to validate the choice of the AAE for biomass burning emissions (Sandradewi et al., 2008a; Zotter et al., 2017).

The AAE_{ff} range in Madrid was estimated from measurements recorded during a specific experiment carried out in traffic hot-spot area. The measurements were made during the early morning rush hours next to a traffic light of a dense traffic lane. AAE_{ff} results were in the range [0.97 – 1.12], coinciding with the lowest percentiles obtained in this study for Escuelas Aguirre and CIEMAT (Fig. S9). These values are consistent with previous findings reported in the literature for fossil fuel emissions (Favez et al., 2009; Titos et al., 2017; Zotter et al., 2017).

Although differences between the Pearson correlation coefficient choosing single values of AAE_{ff} and AAE_{bb} or a range for each of them are less than 1 %, in this work two ranges are proposed to be used for fossil fuel and biomass burning source apportionment, respectively. In the first case, it is considered that the selected range represents more properly all traffic conditions. In the second case, two different values were obtained that maximize the R-Pearson coefficient depending on the selected biomass burning tracers, K_{bb} or organic compounds, thus to be more coherent, the range between both values was chosen.

In the next step, the contributions of fossil fuel and biomass burning of eBC were calculated by means of the Aethalometer model (Eqs. (6) – (9)). They were analyzed in three different ways. In the first method, we set the AAE_{ff} value at the low end of the interval previously obtained, and then we calculated both eBC contributions increasing the AAE_{bb} in increments of 0.01 within the range previously obtained. Then, we increased AAE_{ff} for 0.01 and repeated the same process, progressing successively through all possible combinations of AAE_{ff} and AAE_{bb} in their corresponding intervals: AAE_{ff} = [0.97 – 1.12] and AAE_{bb} = [1.63 – 1.74]. The other two ways consisted of generating random pairs of AAE_{ff} and AAE_{bb} within their corresponding ranges, assuming that the AAE for each source had either a uniform distribution or a Gaussian/normal distribution. The mean (μ) and the standard deviation (σ) assumed for the uniform distribution were μ = 1.045 and σ = 0.043 for AAE_{ff}, and μ = 1.685 and σ = 0.025 for AAE_{bb}.

For the normal distribution, the values were $\mu = 1.045$ and $\sigma = 0.035$ for AAE_{ff}, and $\mu = 1.685$ and $\sigma = 0.018$ for AAE_{bb}.

Finally, the resulting contributions of eBC_{ff} and eBC_{bb} to the total eBC were calculated by averaging all contributions, on the one hand, those of eBC_{ff} and on the other, those of eBC_{bb} previously obtained, with their corresponding standard deviations. The calculations were performed for all the three methods. The difference between the three methods of estimation the eBC_{ff} and eBC_{bb} contributions described above was less than 1%. Therefore, the first way was used in the rest of the work.

To sum up, as in the Madrid site traffic is the main source, especially in summer, and in Villanueva biomass burning is the dominant source during the winter, AAE_{ff} in Madrid (AAE_{ff} = [0.97 – 1.12]) and AAE_{bb} in Villanueva (AAE_{bb} = [1.63 – 1.74]) were taken as the AAE reference values in this work.

3. RESULTS AND DISCUSSION

3.1 eBC mass concentrations and contribution to PM_{10}

Mean eBC values and the corresponding standard deviations obtained at the three sites during the period of study were 3.70 ± 3.73 $\mu g \cdot m^{-3}$ at Escuelas Aguirre, 2.33 ± 2.96 $\mu g \cdot m^{-3}$ at CIEMAT, and 2.61 ± 5.04 $\mu g \cdot m^{-3}$ at Villanueva. The highest mean eBC concentration was recorded, as expected, in Escuelas Aguirre, since it is an urban site highly influenced by traffic. The eBC had a significant seasonal dependence at the three sites (Fig. 2). The most extreme seasonal variation was observed at the rural site Villanueva, where maximum eBC hourly values around 52 $\mu g \cdot m^{-3}$ were recorded in winter, while in summer eBC hourly concentrations never exceeded 16 $\mu g \cdot m^{-3}$.

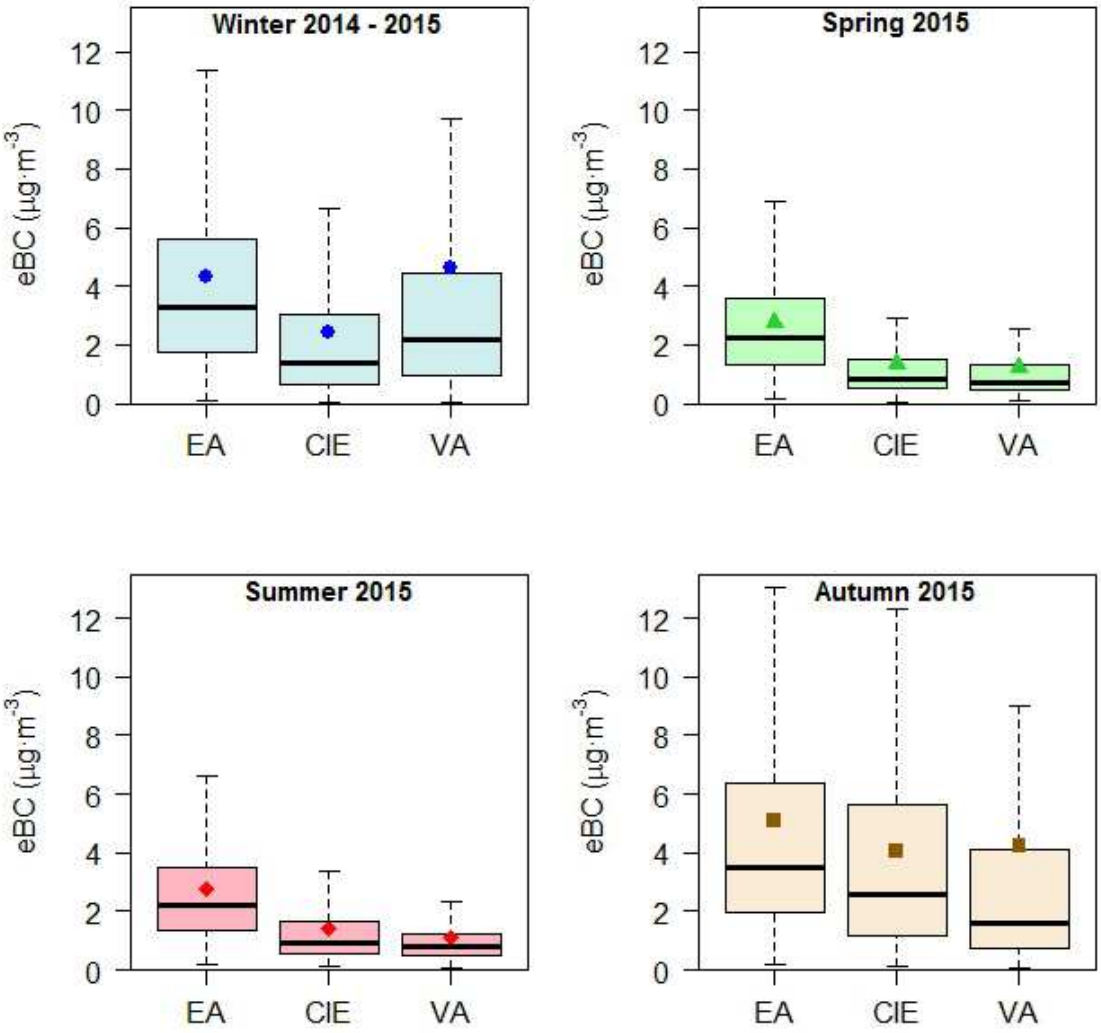

Figure 2. Boxplots of hourly average eBC mass concentrations ($\mu g \cdot m^{-3}$) at the three measurement sites during the four seasons. The central box spans the first quartile to the third quartile. The line inside the box shows the median and "whiskers" above and below the box show the minimum and maximum. Open circles represent extreme high values. The colored markers show the mean. Sites: Escuelas Aguirre (EA), CIEMAT (CIE) and Villanueva del Arzobispo (VA).

The values measured in autumn and winter in Villanueva exceed those typically found in other rural areas in Spain (Querol et al., 2013). Significantly lower values have been measured in different rural areas of Europe, this is because Villanueva is located in a valley with frequent temperature inversions in winter which lead to reduced vertical mixing of the air and to an accumulation of air pollutants within the boundary layer. Additionally, high concentrations may be attributed to the enhanced biomass burning emissions activities in the cold months as discussed later. For instance, in an area 10 km south of the city center of Edinburgh (UK) (Heal and Hammonds, 2014) the eBC (measured by a Diffusion Systems MD43 EEL reflectometer) average concentration was 0.5 $\mu g \cdot m^{-3}$ for a study period of two months

(February to April 2009). In contrast, in some rural regions of Southeast Asia, such as India where biomass burning is a major source, the observed eBC values are significantly higher and close to 10 $\mu g \cdot m^{-3}$ (annual mean value) (Guha et al., 2015) with wintertime average values twice as high compared to the annual average.

In urban areas in Spain, the eBC mean values observed in Barcelona-CSIC (eBC = 2.1 $\mu g \cdot m^{-3}$) and Granada University (eBC = 2.6 $\mu g \cdot m^{-3}$) (Querol et al., 2013; Titos et al., 2015) are similar to those obtained at the Madrid urban background site in this work. However, in other urban sites in Europe lower eBC mean concentrations have been obtained in winter but similar values in summer (Herich et al., 2011; Crilley et al., 2015).

The temporal evolution of the eBC mass concentrations in this study shows that eBC peaks matched the hourly average PM_{10} mass concentration measured at each site in winter and autumn but not necessarily in spring and summer (Figs. S10 – S12 in the Supplementary Information). The relationship can be more closely analyzed by studying the data scatter plots and regression fit results between PM_{10} and eBC. As expected, the linear regression coefficients of determination do not particularly reflect a very high correlation (R^2 = 0.39 at Escuelas Aguirre, R^2 = 0.20 at CIEMAT, and R^2 = 0.55 at Villanueva). However, the correlation between eBC and PM_{10} at the rural site was significantly better than at the urban sites in winter and autumn. The coefficients of determination obtained from the linear regression between eBC and PM_{10} in Villanueva were R^2 = 0.84 in winter and R^2 = 0.72 in autumn. These higher values in these two seasons indicate that eBC and PM_{10} very probably have the same origin in these periods of the year. On the contrary, in spring and summer the values R^2 = 0.10 and R^2 = 0.04, respectively, obtained for this coefficient can be attributed to the influence of a mix of different sources, particularly large amounts of Saharan dust transported to the area, which increased PM_{10} mass concentration without increases in eBC.

Table 1 summarizes the average eBC/PM_{10} ratios for the three sites and for each season. At all sites, the highest values were recorded in autumn and winter. In Madrid, the eBC contributions to the PM_{10} fraction varied from 7 % in summer to 20 % in winter at the background site, whereas this contribution was slightly higher, from 11 % in summer to 21 % in winter, at the traffic-influenced station. These values are consistent with the 3-11 % contribution reported in other European urban background areas and with values up to 24 % found in some European urban traffic stations (Reche et al., 2011) (see Table S1 and references therein). The autumn and winter months seem to be critical in Madrid in the light

of the observed increase in the eBC concentrations. In fact, during the early winter 2014-2015 and late autumn 2015 several pollution episodes took place under anticyclonic stagnant conditions favoring the accumulation of the eBC concentrations mainly derived from traffic emissions (Figures S10 and S11). Nevertheless, the standard deviation values in Table 1 provide a measure of the large variations of the eBC/PM_{10} ratios for each season. Therefore, special conditions such as low PM_{10} concentrations (giving rise to high eBC/PM_{10} ratios) must be taken into account when these ratios are used for comparison purposes.

Table 1. eBC/PM_{10} ratios at Escuelas Aguirre, CIEMAT and Villanueva del Arzobispo for each season during the period of study.

Season	Escuelas Aguirre (Madrid)	CIEMAT (Madrid)	Villanueva del Arzobispo (Jaén)
	eBC/PM_{10}	**eBC/PM_{10}**	**eBC/PM_{10}**
Winter 2014 - 2015	0.21 ± 0.13	0.20 ± 0.14	0.09 ± 0.06
Spring 2015	0.15 ± 0.11	0.10 ± 0.09	0.06 ± 0.07
Summer 2015	0.11 ± 0.08	0.07 ± 0.06	0.04 ± 0.05
Autumn 2015	0.17 ± 0.11	0.19 ± 0.15	0.11 ± 0.10

In the rural area of Villanueva, the eBC contribution to PM_{10} was significantly lower compared to the urban sites, varying from 4 % in the summer to 11 % in the autumn, which is consistent with the 3.6 % value reported at another rural site in Europe (Heal and Hammonds, 2014). The highest contribution was recorded in autumn 2015 and winter 2014-2015. The low eBC content in PM_{10} was affected by the mixture of pollution sources and meteorological conditions. In addition, the different composition of the combustion emissions, the mineral dust sources associated with African dust outbreaks and the formation of secondary inorganic and organic aerosol, mostly from anthropogenic emissions (Salvador et al., 2016), should be considered, which could also increase the concentrations of PM_{10} by non-carbonaceous materials, thereby decreasing the eBC/PM_{10} ratio.

3.2 Source apportionment of eBC

The measured diurnal average cycles of the AAE at Escuelas Aguirre, CIEMAT, and Villanueva during the period of study are shown in Figure 3. The AAE in Villanueva is characterized by a strong diurnal variation during winter and autumn, with values in the evening hours until dawn consistent with an increase of biomass burning activity due to the use of the domestic woodstoves. The AAE average

values in the rural area were 1.80 ± 0.30 in winter and 1.45 ± 0.35 in autumn. During the summer, the AAE was relatively constant throughout the day at all three sites with average values of 1.08 ± 0.05 in Escuelas Aguirre, 1.08 ± 0.13 in CIEMAT, and 1.19 ± 0.15 in Villanueva. Similar relatively flat profiles were measured in Escuelas Aguirre and CIEMAT during the other three seasons, with AAE average values of 1.07 ± 0.09 in winter, 1.05 ± 0.05 in spring and 1.07 ± 0.06 in autumn at Escuelas Aguirre and 1.17 ± 0.08 in winter, 1.16 ± 0.08 in spring and 1.07 ± 0.07 autumn at CIEMAT.

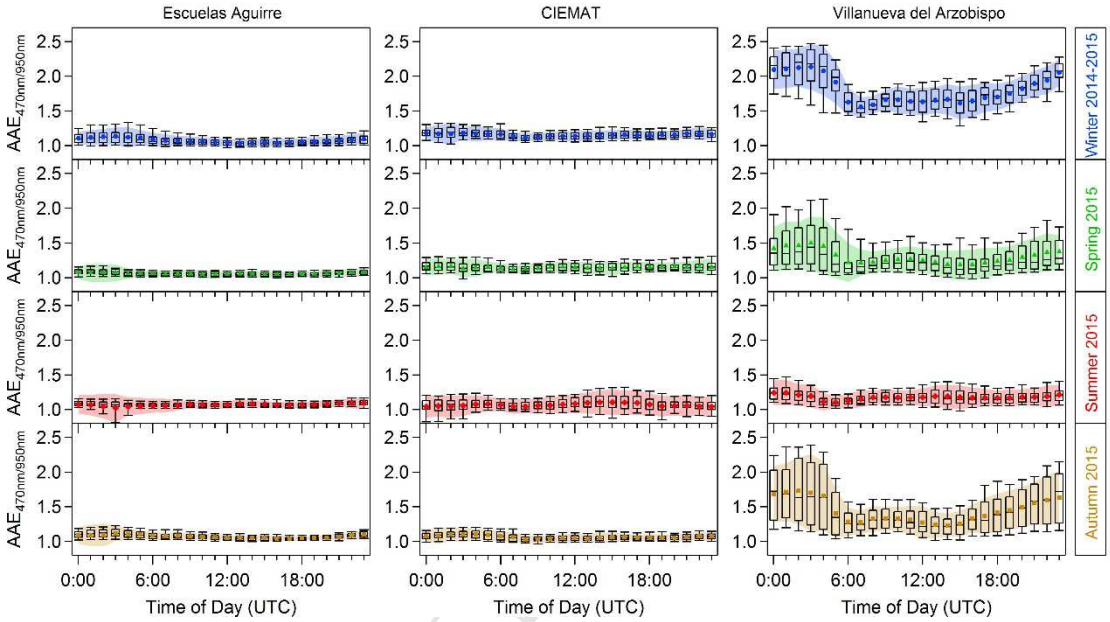

Figure 3. Diurnal average variation of the absorption Ångström exponent at Escuelas Aguirre, CIEMAT and Villanueva del Arzobispo during the four seasons. The central box spans the first quartile to the third quartile. The line inside the box shows the median and "whiskers" above and below the box show the minimum and maximum. The colored markers show the mean values and shadowed areas correspond to the corresponding standard deviation.

The estimated absorption Ångström exponent (AAE) values using the methodology described in the methods section were between 0.97 and 1.12 for fossil fuel and between 1.63 and 1.74 for biomass burning. These AAE values are consistent with previous studies, which have reported AAE values near 1 related to black carbon from traffic emissions and much higher values for biomass burning aerosols (Kirchstetter et al., 2004; Bergstrom et al., 2007; Sandradewi et al., 2008b; Zotter et al., 2017). The source contributions to eBC were determined based on the above source specific AAE values (AAE_{ff} = [0.97 – 1.12] and AAE_{bb} = [1.63 – 1.74]).

The mean eBC_{ff} and eBC_{bb} mass concentrations are shown in Table 2. In Madrid, the mean eBC_{ff} mass concentrations during winter and autumn were up to double and, in some cases, even triple

compared to the other two seasons. The same happened in Villanueva but for eBC_{bb}. In winter, the contribution of the prevailing source at each site seems to be exacerbated by meteorological conditions at each site.

Table 2. Average mass concentration of eBC_{ff} and eBC_{bb} at Escuelas Aguirre, CIEMAT, and Villanueva del Arzobispo sites.

Period	Escuelas Aguirre (Madrid)		CIEMAT (Madrid)		Villanueva del Arzobispo (Jaén)	
	eBC_{ff} ($\mu g \cdot m^{-3}$)	eBC_{bb} ($\mu g \cdot m^{-3}$)	eBC_{ff} ($\mu g \cdot m^{-3}$)	eBC_{bb} ($\mu g \cdot m^{-3}$)	eBC_{ff} ($\mu g \cdot m^{-3}$)	eBC_{bb} ($\mu g \cdot m^{-3}$)
Total period	3.5 ± 3.6	0.2 ± 0.3	2.1 ± 2.7	0.2 ± 0.3	0.9 ± 1.7	1.7 ± 4.2
Winter 2014 – 2015	4.1 ± 4.0	0.2 ± 0.3	2.1 ± 2.5	0.3 ± 0.4	0.5 ± 1.2	4.1 ± 6.0
Spring 2015	2.7 ± 2.1	0.1 ± 0.1	1.2 ± 1.5	0.2 ± 0.2	0.8 ± 1.0	0.4 ± 1.0
Summer 2015	2.6 ± 2.2	0.1 ± 0.2	1.3 ± 1.5	0.1 ± 0.3	0.9 ± 1.2	0.2 ± 0.4
Autumn 2015	4.9 ± 5.0	0.2 ± 0.2	3.8 ± 3.9	0.2 ± 0.3	1.5 ± 2.6	2.7 ± 5.4

The average diurnal cycles of eBC_{ff} and eBC_{bb} are summarized in Figures 4 to 7 (stacked area charts in this case) for each season for all three sites. For the Madrid sites, the eBC_{ff} is practically the same as that of the total measured eBC. During weekdays, the eBC_{ff} concentration in Escuelas Aguirre and Villanueva was characterized by two peaks, one in the morning and another in the late afternoon/early evening, coinciding with peak traffic times. On the contrary, the eBC_{ff} in the urban background site in CIEMAT had only one major peak in the morning. The evening peak was also present but quite weak. In Madrid, especially in Escuelas Aguirre, on Saturdays and on Sundays the evening eBC_{ff} peak is higher than the morning one. This is related to nightlife activities in Madrid and people returning home after the weekend, respectively.

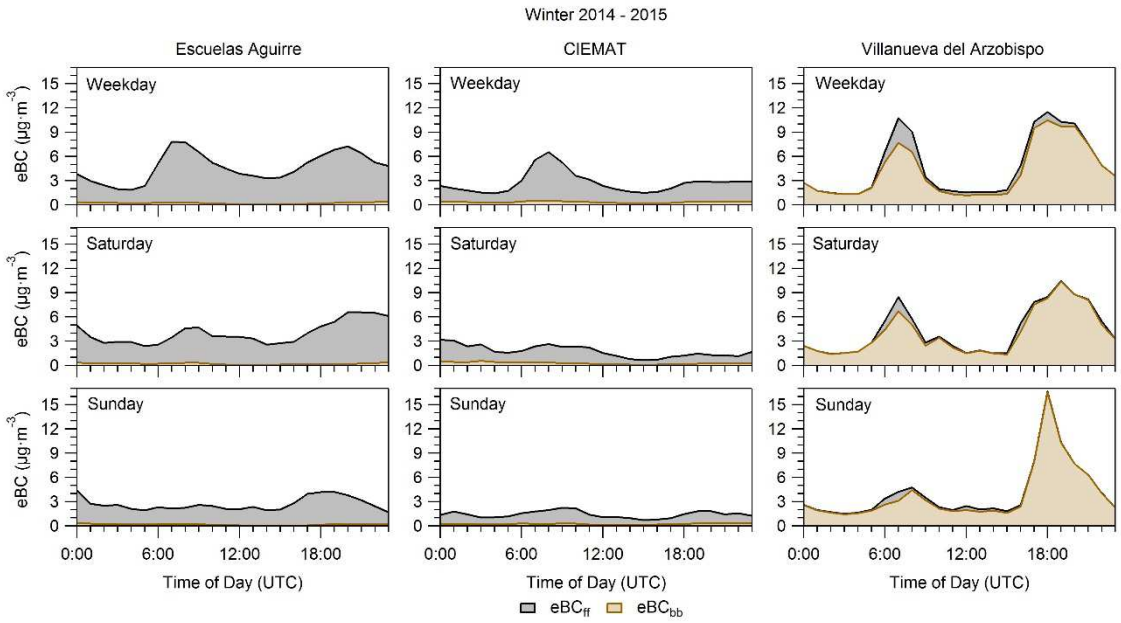

485

486 **Figure 4.** Average diurnal profiles of eBC source apportionment from fossil fuel (gray area) and biomass
487 burning (brown area) for Escuelas Aguirre, CIEMAT and Villanueva del Arzobispo on weekdays (first
488 line), Saturdays (second line), and Sundays (third line) during the winter of 2014–2015.

489

490

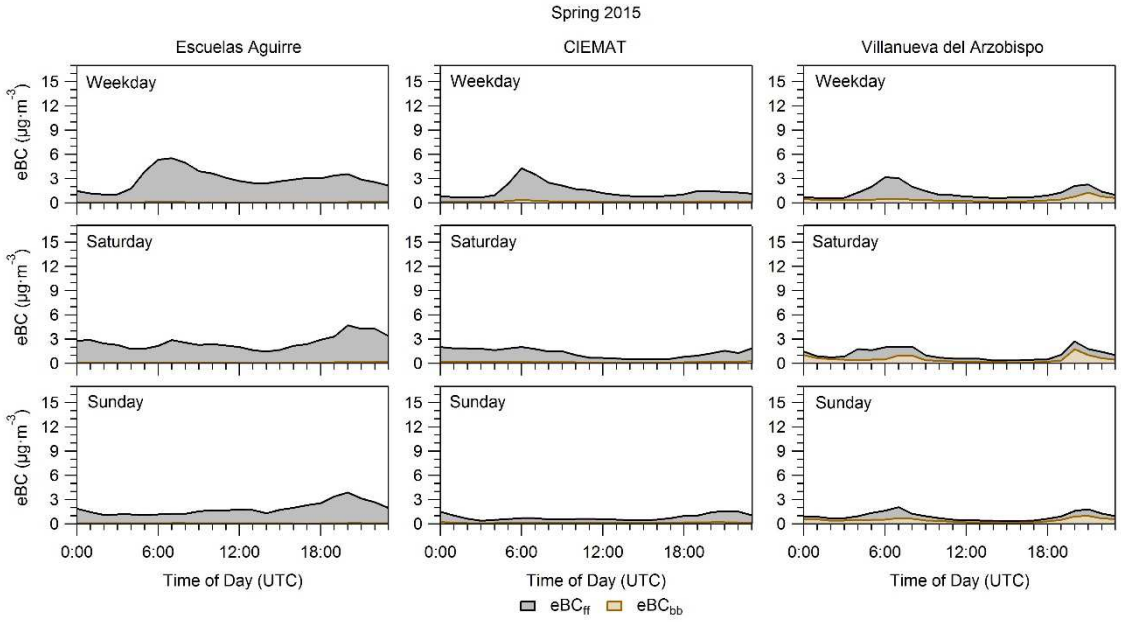

491

492 **Figure 5.** Average diurnal profiles of eBC source apportionment from fossil fuel (gray area) and biomass
493 burning (brown area) for Escuelas Aguirre, CIEMAT and Villanueva del Arzobispo on weekdays (first
494 line), Saturdays (second line), and Sundays (third line) during the spring of 2015.

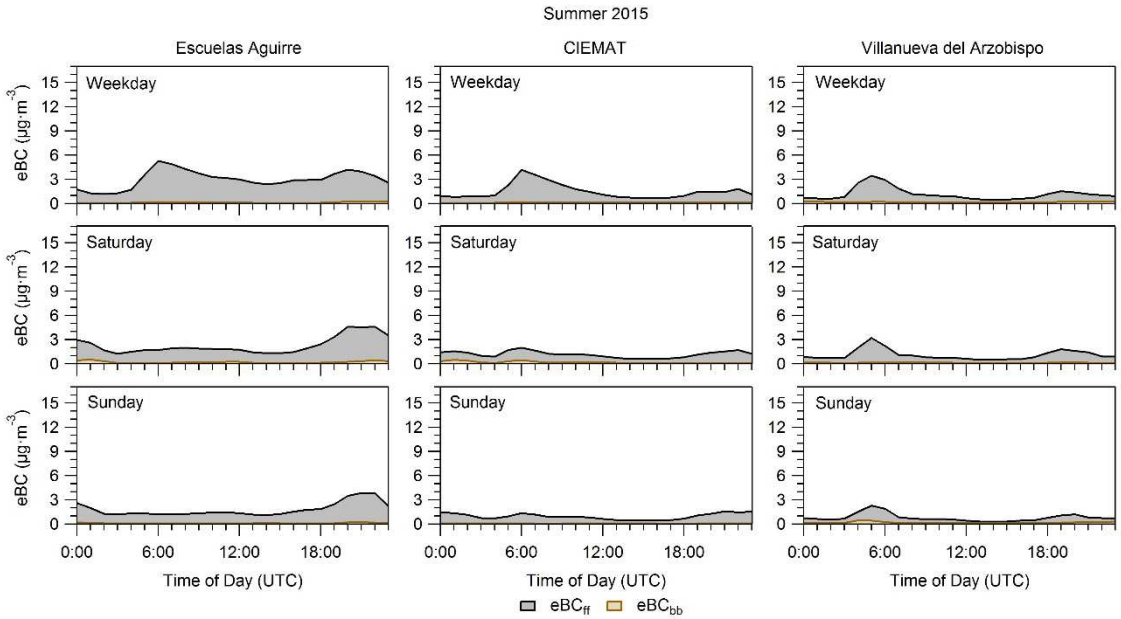

Figure 6. Average diurnal profiles of eBC source apportionment from fossil fuel (gray area) and biomass burning (brown area) for Escuelas Aguirre, CIEMAT and Villanueva del Arzobispo on weekdays (first line), Saturdays (second line), and Sundays (third line) during the summer of 2015.

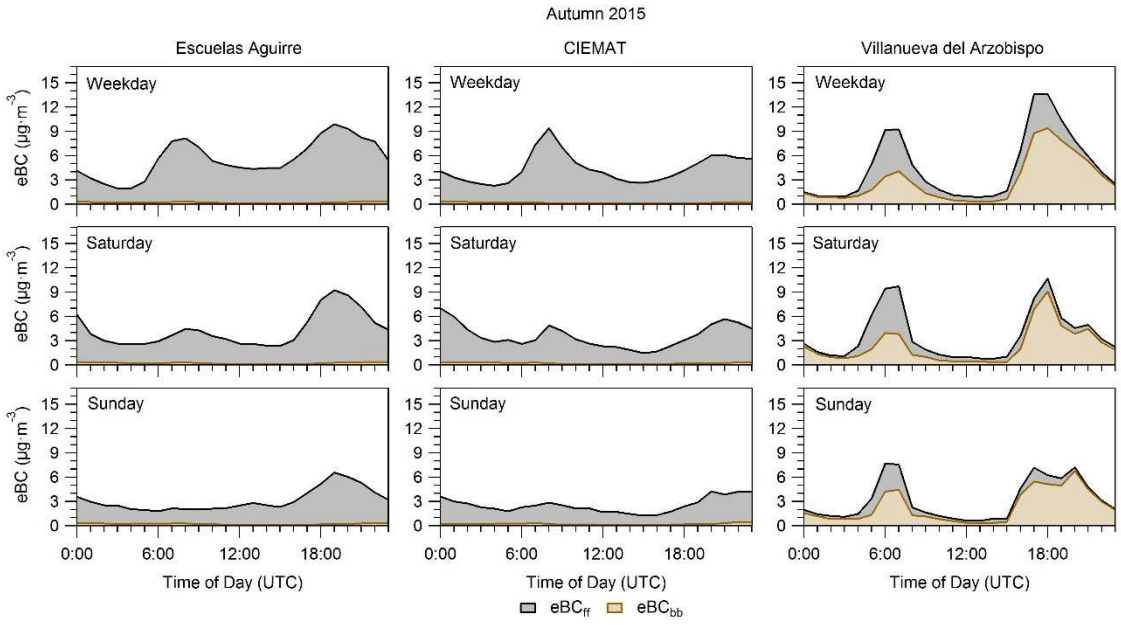

Figure 7. Average diurnal profiles of eBC source apportionment from fossil fuel (gray area) and biomass burning (brown area) for Escuelas Aguirre, CIEMAT and Villanueva del Arzobispo on weekdays (first line), Saturdays (second line), and Sundays (third line) during the autumn of 2015.

The average diurnal cycle of eBC_{bb} in Villanueva, in the winter and in the autumn, was characterized by a strong early evening peak and a relatively weak morning peak (Figs. 4 and 7). Some

differences are observed between both seasons, in winter the contribution of eBC_{bb} is higher during the traffic rush-hours comparing to autumn peaks, especially during evenings and nights which can be explained by the typical operating time pattern of domestic heating appliances in the coldest months. The Sunday nighttime eBC was stronger in winter than the other days and was observed a couple of hours earlier than during the rest of the week consistent with the different activity schedule followed by people on Sundays. In contrast, during the spring and the summer, due to the absence of operation of domestic stoves, eBC concentrations are predominantly resulting from traffic emissions and the contribution of eBC_{bb} to total eBC is practically negligible except for the morning and evening/night hours in spring. In addition, due to the change of local time in March and October, a small displacement of the peaks is observed between winter and autumn and between summer and spring.

More than 93 % of the eBC in the traffic site in Madrid was due to fossil fuel emissions during all seasons (Table 3). The traffic contribution at CIEMAT was a little lower but still represented more than 84 % of the eBC in this urban background site. The highest biomass burning contribution to eBC in CIEMAT was 16 % during the winter. These results indicate that biomass burning contributed little to the eBC levels in Madrid in all seasons and confirm that fossil fuel combustion was the dominant source. This is the first time that these results are obtained for the city, and, comparing them with other cities, the values reported here for the fraction of eBC_{bb} in winter (7 % in Escuelas Aguirre and 16 % at CIEMAT) are lower compared to those obtained in the same season for urban site in Zürich (25%) (Herich et al., 2011), yet similar to those observed for urban sites in Paris (15%) (Healy et al., 2012) and London (15%) (Crilley et al., 2015).

Table 3. Percent contribution of eBC_{ff} and eBC_{bb} to total eBC at Escuelas Aguirre, CIEMAT, and Villanueva del Arzobispo sites.

Season	Escuelas Aguirre (Madrid)		CIEMAT (Madrid)		Villanueva del Arzobispo (Jaén)	
	eBC_{ff}	eBC_{bb}	eBC_{ff}	eBC_{bb}	eBC_{ff}	eBC_{bb}
Winter 2014 – 2015	93 ± 20	7 ± 9	84 ± 38	16 ± 11	12 ± 18	88 ± 43
Spring 2015	96 ± 21	4 ± 4	85 ± 36	15 ± 11	64 ± 37	36 ± 32
Summer 2015	95 ± 17	5 ± 6	91 ± 23	9 ± 12	81 ± 20	19 ± 18
Autumn 2015	95 ± 25	5 ± 6	95 ± 20	5 ± 6	50 ± 37	50 ± 37

The situation was quite different in the rural area (Villanueva) where biomass burning was a significant source of eBC in all seasons but summer. It was estimated that biomass combustion

contributed 88 % of the eBC during the winter and to be a significant source during the autumn (50 %) and the spring (36 %) (Table 3). At this site, it is also the first time that such results are obtained. The values obtained in this work for eBC_{bb} are much higher than those observed for rural areas in the UK (30 % in winter) (Crilley et al., 2015) and in Switzerland (33 % in winter and 6 % in summer) (Herich et al., 2011). The eBC due to biomass burning was more similar to the small village of Roveredo, in an Alpine valley of Switzerland (51% in winter) (Sandradewi et al., 2008a). The polar plot in Figure S13 shows, as an example, the mean concentrations of the contributions of eBC_{ff} and eBC_{bb} to the total eBC in relation to the wind direction and wind speed obtained during the autumn in Villanueva. It can be seen that higher concentrations were associated to South wind direction with the maximum values at lower wind speeds, indicating that the corresponding sources are mainly of local origin. It should be noted that Villanueva is located in a valley formed by two rivers and a lot of winter thermal inversions occur in the area.

3.3 eBC, EC and OC comparison

Figure 8 shows the slopes (± standard error) and the correlation of the linear regression through the origin between total eBC mass concentrations from the Aethalometer and EC mass concentration in PM_{10} in both sites CIEMAT and Villanueva. The difference between the slopes needs to be interpreted with care as the number of samples at CIEMAT is smaller (n = 20) and all samples are PM_{10} (including different amounts of mineral matter, possibly interfering with the thermal analysis), and may be statistically biased. The difference may be mainly due to the distinct aerosol chemical composition by the sources at each site, besides their age in the atmosphere influencing the coating of the black carbon cores.

EC and OC at CIEMAT were strongly correlated with eBC and eBC_{ff} and a weaker correlation was obtained for eBC_{bb} (Figure. 8 (top) and 9 (top)), suggesting the lower influence of biomass burning source at this location. In Villanueva, EC and OC were also highly correlated, but as opposed to the urban area, with the total eBC and eBC_{bb} mass concentrations and weaker with eBC_{ff} (Figures. 8 (bottom) and 9 (bottom)), indicating that the main source at this site is biomass burning (see supplement Figure S14, correlation in winter 2014 – 2015 and spring 2015). It should be noted that, in contrast to Zotter et al., (2017), EC was not source apportioned in this work.

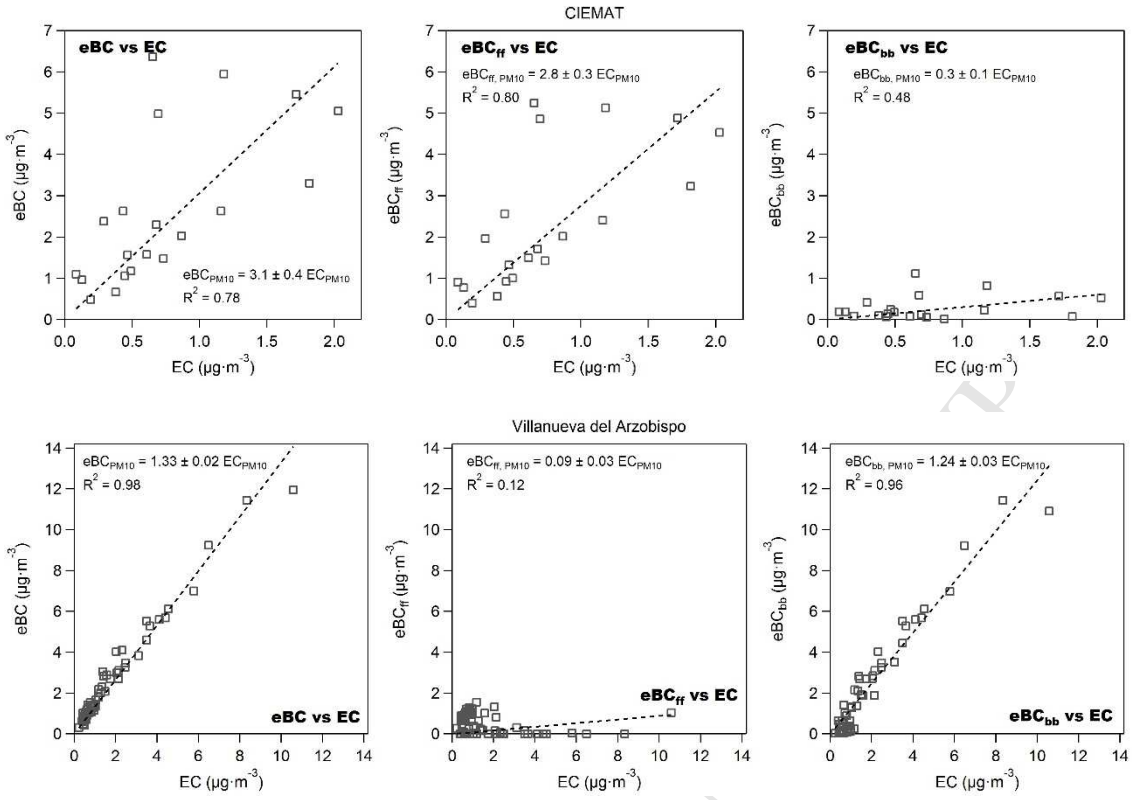

561

562

563 **Figure 8.** Relationship between eBC and EC mass concentrations in PM_{10} collected at CIEMAT (n = 20,
564 top) and Villanueva del Arzobispo (n = 59, bottom).

565

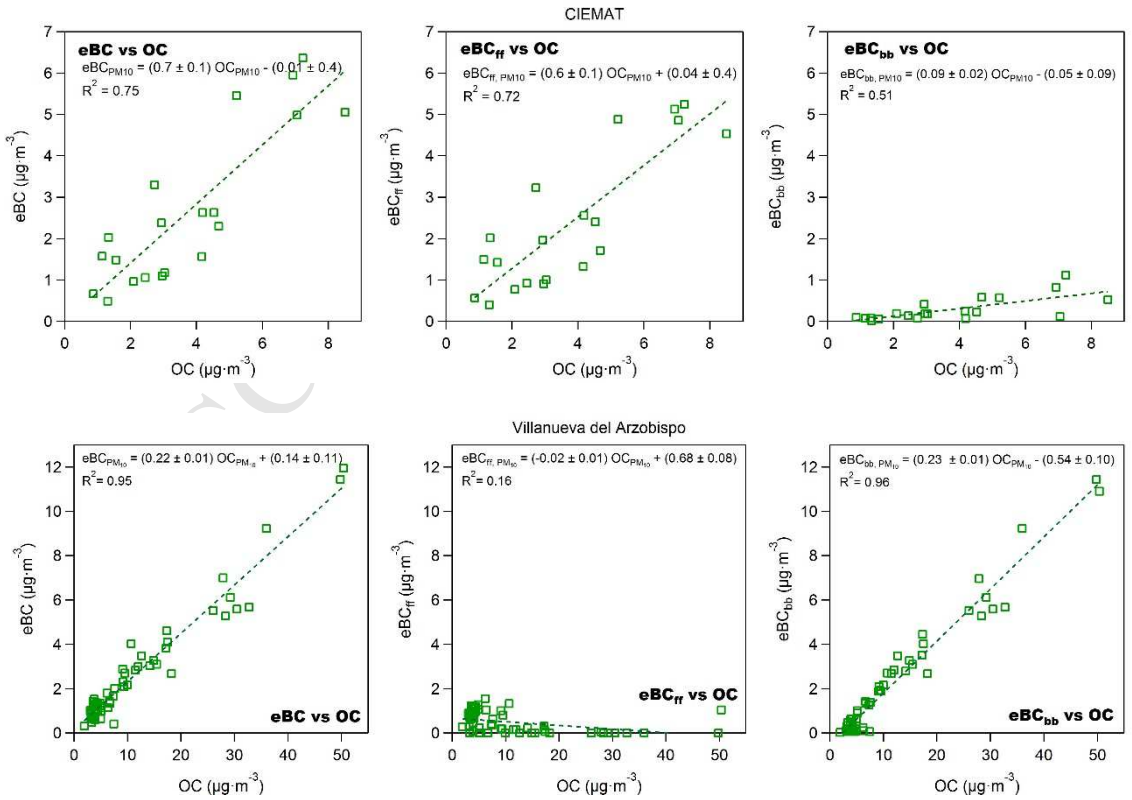

566

567

568 **Figure 9.** Relationship between eBC and OC mass concentrations in PM_{10} collected at CIEMAT (n = 20,
569 top) and Villanueva del Arzobispo (n = 59, bottom).

570

571 MAC values of 13.3 ± 1.6 $m^2 \cdot g^{-1}$ at CIEMAT (from November 20, 2014 to June 30, 2015; n =
572 20) and 5.87 ± 0.1 $m^2 \cdot g^{-1}$ at Villanueva (from November 22, 2014 to June 29, 2015; n = 59) were
573 obtained at a wavelength of 950 nm from the linear regression through the origin between b_{abs} (950nm)
574 and EC (not shown here). The correlation coefficients (R^2) were 0.78 in CIEMAT and 0.98 in Villanueva,
575 showing strong correlation at both sites. The large difference in MAC values could be due to EC being
576 removed from the filter during the helium phase of the analysis. It has been documented that in samples
577 where the amount of EC is small (below or near the detection limit), a bias may occur in the position of
578 the Sunset OCEC split and result in inaccurate EC values (Bae et al., 2004; Arhami et al., 2006; Bauer et
579 al., 2009). If EC is "artificially" low, then MAC needs to be higher to achieve eBC. Moreover, it is
580 necessary to take into account the fact that all samples are PM_{10}, which indicates contribution of mineral
581 dust on the coarser fraction of ambient particle concentrations (Artíñano et al., 2003; Zanatta et al., 2016).
582 These MAC values are in contrast to the finding of Zotter et al., (2017), where results indicate no
583 significant difference in MAC at 880 nm (with a value of 11.8 $m^2 \cdot g^{-1}$) between eBC originating from
584 traffic or wood-burning emissions. Therefore, further analyses of EC are required.

585 OC and EC concentrations obtained at CIEMAT in this study (see Table S2) were similar to
586 those reported by Plaza et al. (2011) at the same place, except for very low EC values, as mentioned
587 above. A seasonal variation was observed in the EC values at CIEMAT and Villanueva (Tables S2 and
588 S3) showing a decrease in the spring period, which could be related to favorable atmospheric dilution
589 conditions and reduction of emissions. Maximum EC and OC values, which occurred in winter, can be
590 associated to meteorological conditions causing pollutant accumulation close within the surface layer,
591 especially during periods of atmospheric stagnation.

592 The OC/EC mass ratios can be used to study the emission and transmission characteristics of
593 carbonaceous aerosol, which due to the source variability for a specific site, can have a seasonal character
594 throughout the year (see Tables S1 and S2). In general, OC/EC ratios in many urban sites around the
595 world are in the range of 1.0 to 4.0, a value greater than 2.0 is attributed to SOA formation in the
596 atmosphere (Cao, 2003). However, such high OC/EC ratios cannot be explained only in terms of
597 enhanced contribution from SOA, rather it can be associated to the predominance of biomass burning
598 sources (Ram and Sarin, 2010). Plaza et al. (2011) obtained at CIEMAT monthly averaged OC/EC ratios
599 ranged from 1.6 to 6.0. In the aforementioned study, a seasonal variation was observed with lower values

in winter and higher values in spring-summer. In our work, OC/EC ratio ranged at CIEMAT from 1.3 to 26.5 in PM_1, from 1.5 to 26.5 in $PM_{2.5}$ and from 1.5 to 34.5 in PM_{10}, and in Villanueva from 3.5 to 18.4 in $PM_{2.5}$ and from 3.6 to 15.5 in PM_{10}. In the urban area, the ratios showed weak correlations (R^2 = 0.11 in PM_1 and in $PM_{2.5}$, and R^2 = 0.27 in PM_{10}). In the rural station, the high ratios of OC/EC have been explained by the presence of local sources such as biomass burning combustion (Na et al., 2004; Zhang et al., 2007), showing a preponderance of OC. In other rural sites in Europe, similar OC/EC ratios to those in Villanueva have been observed (Castro et al., 1999; Pio et al., 2007, 2011; Sandrini et al., 2014). At these sites, the increase of OC concentrations in winter has been related to biomass burning for residential heating and a similar origin could be deduced for Villanueva. The slopes and their standard errors of the linear regression between OC and EC at this site were 5.5 ± 0.2 in $PM_{2.5}$ and 5.6 ± 0.2 in PM_{10}, showing a high correlation both in $PM_{2.5}$ (R^2 = 0.91) and PM_{10} (R^2 = 0.94) (see Fig. 10). The intercept (1.1 ± 0.6 in $PM_{2.5}$ and 1.3 ± 0.6 in PM_{10}) can be interpreted as the OC background concentration from non-combustion sources, however, it can be biased by uncertainty in carbon measurement. Nevertheless, it may also be understood as the biogenic secondary organic aerosol source found by Salvador et al., (2016) after a source apportionment study performed at this same site. The high OC/EC ratios obtained in Villanueva, their seasonal behavior with higher values in winter, and the good correlation between OC and EC that suggests they have come common sources, allowed to conclude that the main contribution to atmospheric particles derived from biomass burning.

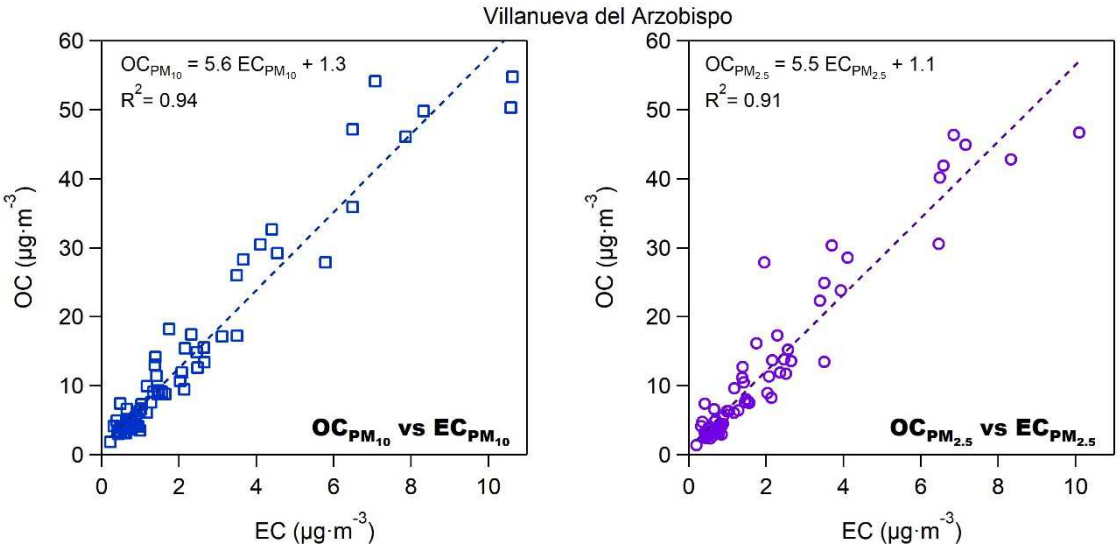

Figure 10. Relationship between OC and EC mass concentrations in PM_{10} (left) and $PM_{2.5}$ (right) collected from 22th November 2014 until 29th June 2015 in Villanueva del Arzobispo (n = 59).

3.4 eBC and biomass burning tracers

The concentrations of three monosaccharide anhydrides (MAs) (levoglucosan, mannosan and galactosan) that are often used as biomass burning tracers together with the potassium associated with biomass burning (K_{bb}) were measured in Villanueva. Winter and spring average mass concentrations are shown in Table 4. The levoglucosan and K_{bb} concentrations in winter increased up to 5.9 $\mu g \cdot m^{-3}$ and 5.6 $\mu g \cdot m^{-3}$ in $PM_{2.5}$ and 7.4 $\mu g \cdot m^{-3}$ and 6.3 $\mu g \cdot m^{-3}$ in PM_{10}, respectively, at times when the impact of biomass burning emissions is expected to be higher. In the same season, concentrations of mannosan varied from 0.01 to 0.38 $\mu g \cdot m^{-3}$ in $PM_{2.5}$ and from 0.01 to 0.47 $\mu g \cdot m^{-3}$ in PM_{10}, and those of galactosan from 0.01 to 0.30 $\mu g \cdot m^{-3}$ in $PM_{2.5}$ and from 0.01 to 0.36 $\mu g \cdot m^{-3}$ in PM_{10}. Levoglucosan concentrations measured in Villanueva are in the range of values reported for other areas such as Aveiro in Portugal (Gelencsér et al., 2007; Puxbaum et al., 2007) and Fresno in US (Schauer and Cass, 2000); but lower than measured concentrations in a rural background site in Italy (Gilardoni et al., 2011) and higher than measured at two rural sites in UK (Crilley et al., 2015) and a rural background site in the Czech Republic (Herich et al., 2014; Schwarz et al., 2016). The concentrations of the MAs are in the range of values reported in Fourtziou et al. (2017). The K_{bb} concentrations were significantly higher compared with values obtained in other rural sites (Harrison et al., 2012; Puxbaum et al., 2007).

Table 4. Average mass concentration of the potassium associated with biomass burning (K_{bb}) and the three organic compounds (levoglucosan, mannosan and galactosan) that are often used as biomass burning tracers and their ratios for winter and spring in Villanueva del Arzobispo.

Season	K_{bb} ($\mu g \cdot m^{-3}$)	L ($\mu g \cdot m^{-3}$)	M ($\mu g \cdot m^{-3}$)	G ($\mu g \cdot m^{-3}$)	L/M	L/G	K_{bb}/L
				PM_{10}			
Winter 2014 – 2015	2.5 ± 1.6	1.7 ± 1.7	0.1 ± 0.1	0.1 ± 0.1	13.2 ± 8.9	18.0 ± 13.1	2.0 ± 1.1
Spring 2015	0.3 ± 0.3	0.1 ± 0.2	0.01 ± 0.01	0.003 ± 0.004	11.0 ± 5.7	24.6 ± 42.8	23.8 ± 31.0
				$PM_{2.5}$			
Winter 2014 – 2015	2.3 ± 1.5	1.4 ± 1.5	0.1 ± 0.1	0.1 ± 0.1	13.5 ± 7.5	20.2 ± 14.6	2.3 ± 1.5
Spring 2015	0.3 ± 0.3	0.1 ± 0.2	0.01 ± 0.01	0.003 ± 0.002	11.7 ± 5.8	28.0 ± 42.3	20.3 ± 23.2

K_{bb} = potassium associated with biomass burning, L= levoglucosan, M = mannosan, G = galactosan

The relationships between the concentrations of these MAs together with K_{bb} and of eBC_{bb} were used in the previous section as a test of the source apportionment algorithm to obtain the best AAE

values. The R^2 coefficient between daily average (24-hour) eBC_{bb} mass concentrations and those of the biomass burning tracers range from 0.71 for levoglucosan, to 0.73 for mannosan, 0.82 for galoctosan, and 0.92 for K_{bb} during winter in Villanueva (Fig. 11, Figs. S15 – S16 and Table S4). The corresponding R^2 values between the eBC_{ff} and these tracers were all much lower and below 0.40. The regression intercept of the four biomass tracers to eBC_{bb} should be zero if the methods are consistent and all species experience the same rate of atmospheric removal (Fuller et al., 2014). In this work, the intercepts were close to zero (Fig. 11), suggesting the stability of the biomass burning tracers during the cold season.

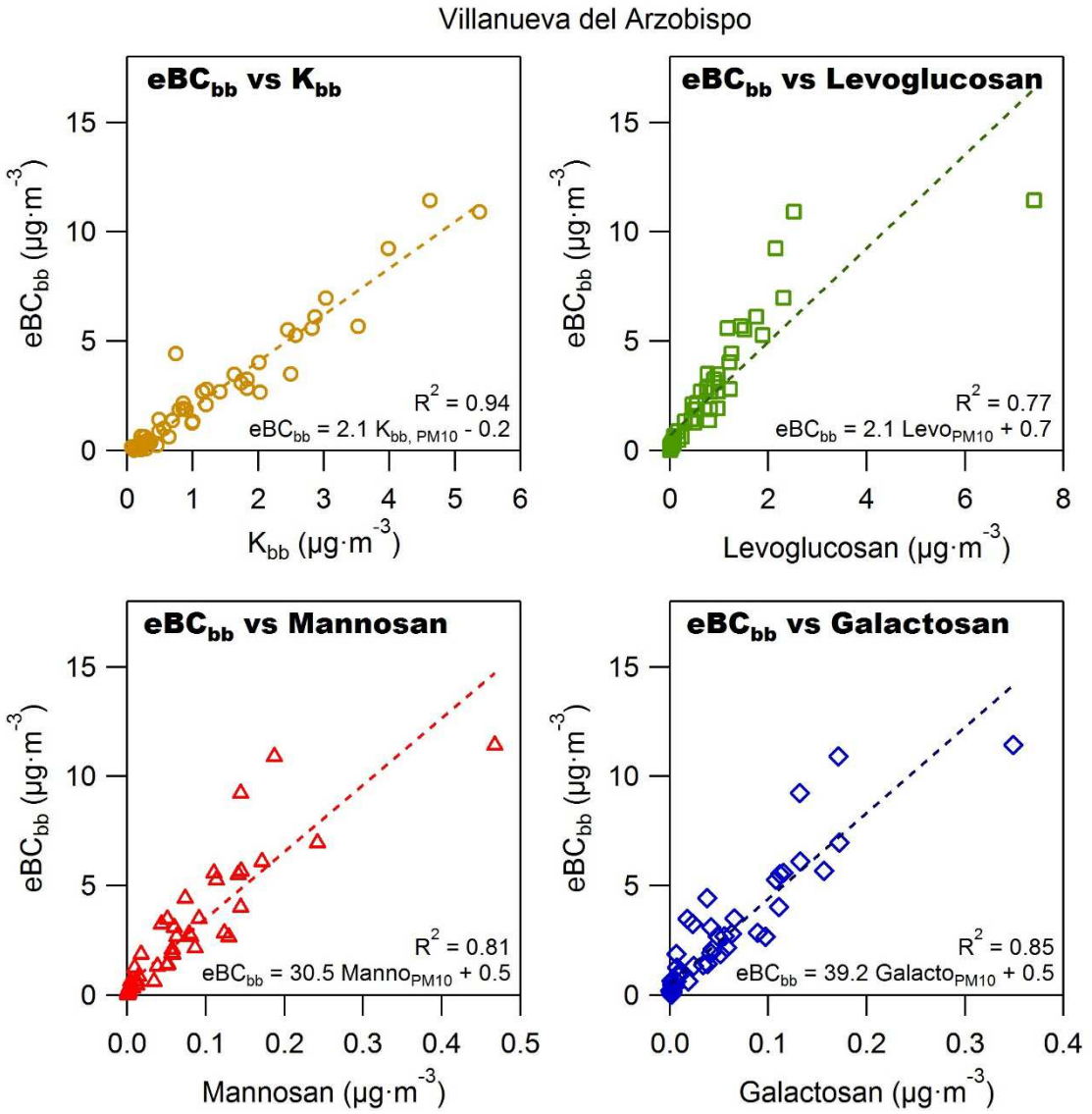

Figure 11. Relationship between eBC_{bb} and the four organic compounds used as biomass burning tracers in PM_{10} collected from 22nd November 2014 until 29th June 2015 in Villanueva del Arzobispo (n = 59). eBC_{bb} vs K_{bb} (open circles, top left), eBC_{bb} vs levoglucosan (open squares, top right), eBC_{bb} vs mannosan (open triangles, bottom left), and eBC_{bb} vs galactosan (open diamonds, bottom right).

The levoglucosan to mannosan (L/M) and the levoglucosan to the sum of mannosan and galactosan (L/(M+G)) ratios can be used to distinguish hard- and soft wood types (Schmidl et al., 2008) and were used before to separate different biomass burning sources (Fabbri et al., 2009; Oanh et al., 2011; Harrison et al., 2012). Hardwood burning leads to high ratios, around 12 – 24, while softwood burning leads to low ratios, around 3 – 7 (Fine et al., 2004; Caseiro et al., 2009). Fabbri et al. (2009) found L/(M+G) ratios larger than 30 for lignite combustion and between 0.4 and 18 for various source tests for biomass burning. These results may be utilized to distinguish the smoke emissions from different fuel types, but those authors recommend being careful when interpreting sources of anhydrosaccharides in atmospheric aerosols due to possible mixing of smoke from burning of lignite and biomass, and due to the high values of the L/M and L/(M+G) ratios for some hardwoods and grasses. The ratio of K_{bb}/L is quite variable between season and sites. Gao et al. (2003) found that the potassium/levoglucosan ratio in aerosols produced from Savannah forest fires was 33.3 during flaming phase and from 0.2 to 0.6 for smoldering combustion. Puxbaum et al. (2007) found winter values of K/L ratio between 0.2 and 2.1 and summer values of 3.3 – 9 at CARBOSOL sites.

In Villanueva, the average L/M ratios in $PM_{2.5}$ were 13.5 ± 7.5 in winter and 11.7 ± 5.8 in spring. The ratios in PM_{10} were quite similar to those in the fine particles: 13.2 ± 8.9 in winter and 11.0 ± 5.7 in spring. The winter and spring average L/(M+G) ratios were 8.0 ± 4.8 and 7.0 ± 5.5 in $PM_{2.5}$ and 7.5 ± 5.2 and 6.4 ± 5.1 in PM_{10}. These values are similar to those ratios that have been found during hardwood combustion in previous studies (Fine et al., 2004; Engling et al., 2006) supporting the hypothesis that the olive wood (one of the hardest of all woods) combustion is a major source of carbonaceous particulate matter at this site. Moreover, these values were much smaller than those reported for lignite burning by Fabbri et al. (2009), suggesting that lignite burning is not considered as a possible source of MAs and the biomass (especially wood) burning is supposed to be the dominant source of MAs found in this area. Relatively high K_{bb}/L ratios were obtained in Villanueva (2.3 ± 1.5 ($PM_{2.5}$) and 2.0 ± 1.1 (PM_{10}) in winter and 20.3 ± 23.2 ($PM_{2.5}$) and 23.8 ± 31.0 (PM_{10}) in spring) in comparison with background sites in Europe (Puxbaum et al., 2007). This may be due to uncertainties introduced by the correction approach described in section 2.2.3, which could lead to an overestimation of potassium associated with biomass burning. Therefore, further analyses of K_{bb} are needed.

4. CONCLUSIONS

Three multi-wavelength Aethalometer measurements were used to study mass equivalent black carbon (eBC) characteristics at two urban sites in Madrid (a background station (CIEMAT) and a traffic site (Escuelas Aguirre)) and in a rural area (Villanueva del Arzobispo) during a full year. The eBC mass concentrations presented concentrations typical of other urban sites, and higher than other rural sites in Europe. They show seasonal variations at the three stations, significantly higher in winter and autumn than in spring and summer, especially at the rural site. This behavior is the result of meteorological conditions during the experimental period but can be also linked to the seasonal variations in emissions, especially high in winter at the rural site due to biomass burning. The highest eBC/PM_{10} ratios were recorded in autumn and winter at the three sites. In Madrid, the highest average eBC contribution to PM_{10} was observed in winter at the urban traffic site (21 %). In those cold months, there was an increase in the eBC concentrations mostly from traffic emissions due to several pollution episodes. In the rural area, the highest eBC/PM_{10} ratio (11 %) also occurred in the cold months, although it was significantly lower compared to the urban sites because of the different composition of the combustion emissions, the mineral dust sources associated with African dust outbreaks and the formation of secondary inorganic and organic aerosol, which could increase the concentrations of PM_{10} with non-carbonaceous materials, thereby decreasing the eBC/PM_{10} ratio.

A sensitivity analysis was performed to estimate the most appropriated AAE values for source apportionment in order to optimize the Aethalometer model and provide realistic results with AAE values between 0.97 and 1.12 for fossil fuel combustion and between 1.63 and 1.74 for biomass combustion. Based on these values, a source apportionment study was performed and fossil fuel combustion was found to be responsible for more than 84 % of the eBC in Madrid in all seasons and also during the warm months in Villanueva del Arzobispo. However, biomass burning contributed 88 % of the total eBC concentration in Villanueva del Arzobispo in the cold months and was also a significant eBC source in autumn (50 %) and spring (36 %).

The measured eBC concentrations were highly correlated with the elemental carbon (EC) and organic carbon (OC) mass concentrations both in CIEMAT and Villanueva del Arzobispo. High correlation between eBC_{ff} with EC and OC and weaker correlation between eBC_{bb} and EC at CIEMAT, showed the low biomass burning influence in Madrid. On the contrary, the strong correlations between eBC_{bb} with EC and OC in the rural area confirmed that the main source is biomass burning. The high

ratios of OC/EC obtained in rural stations can be explained by the presence of local sources such as biomass burning combustion, showing a preponderance of OC. The good correlation between OC and EC suggests they have common sources and showed that the main contribution to atmospheric particles derived from biomass burning.

The high concentration of the biomass burning tracers in Villanueva during winter confirm that the biomass burning is an important source of absorbing aerosols during the cold season. The estimated eBC contribution from biomass burning in the rural station was well correlated with the concentrations of organic biomass burning tracers and very well with the concentrations of the potassium associated with biomass burning, so supporting the applied methodology. Hardwood combustion (most probable olive wood) was the main biomass burning organic aerosol source in Villanueva del Arzobispo based on the measured levoglucosan to mannosan and levoglucosan to the sum of mannosan and galactosan ratios. Relatively high potassium/levoglucosan ratios were obtained.

The proposed methodology has proved to be a valid analytical tool to adequately determine absorption Ångström exponents, which may vary depending on the site and the season. Source apportionment studies based on the Aethalometer model could identify the main sources and their contributions with high temporal resolution. This allows adopting measurements and designing strategies to reduce the eBC concentrations, especially under unfavorable weather conditions or in areas where the source contribution clearly highlights a source, as in rural areas with high domestic use of biomass.

Acknowledgements

This work has been funded by the Spanish Ministry of Economy and Competitiveness (MINECO) through the FPI predoctoral research grant BES-2012-056545 and the MICROSOL (CGL2011-27020) and PROACLIM (CGL2014-52877R) projects. AEROCLIMA project (CIVP16A1811, Fundación Ramón Areces) and the Spanish Ministry of Agriculture, Food and Environment are also acknowledged as well as the Air Quality Service of Junta de Andalucía and the Madrid Authority technical staff for their support in the experimental deployment and measurements.

References

Abdeen, Z., Qasrawi, R., Heo, J., Wu, B., Shpund, J., Vanger, A., Sharf, G., Moise, T., Brenner, S., Nassar, K., Saleh, R., Al-Mahasneh, Q.M., Sarnat, J.A., Schauer, J.J., 2014. Spatial and temporal variation in fine particulate matter mass and chemical composition: The middle east consortium for

aerosol research study. Sci. World J. 2014, 1–16.

Alastuey, A., Querol, X., Aas, W., Lucarelli, F., Pérez, N., Moreno, T., Cavalli, F., Areskoug, H., Balan, V., Catrambone, M., Ceburnis, D., Cerro, J.C., Conil, S., Gevorgyan, L., Hueglin, C., Imre, K., Jaffrezo, J.-L., Leeson, S.R., Mihalopoulos, N., Mitosinkova, M., O'Dowd, C.D., Pey, J., Putaud, J.-P., Riffault, V., Ripoll, A., Sciare, J., Sellegri, K., Spindler, G., Yttri, K.E., 2016. Geochemistry of PM10 over Europe during the EMEP intensive measurement periods in summer 2012 and winter 2013. Atmos. Chem. Phys. 16, 6107–6129.

Albrecht, B.A., 1989. Aerosols, Cloud Microphysics, and Fractional Cloudiness. Science. 245, 1227–1230.

Alier, M., van Drooge, B.L., Dall'Osto, M., Querol, X., Grimalt, J.O., Tauler, R., 2013. Source apportionment of submicron organic aerosol at an urban background and a road site in Barcelona (Spain) during SAPUSS. Atmos. Chem. Phys. 13, 10353–10371.

Alves, C., 2008. Characterisation of solvent extractable organic constituents in atmospheric particulate matter: An overview. An. Acad. Bras. Cienc. 80, 21–82.

Andreae, M.O., 1983. Soot carbon and excess fine potassium: Long-range transport of combustion-derived aerosols. Science. 220, 1148–1151.

Andreae, M.O., Andreae, T.W., Annegarn, H., Beer, J., Cachier, H., Le Canut, P., Elbert, W., Maenhaut, W., Salma, I., Wienhold, F.G., Zenker, T., 1998. Airborne studies of aerosol emissions from savanna fires in southern Africa: 2. Aerosol chemical composition. J. Geophys. Res. Atmos. 103, 32119–32128.

Ångström, A., 1929. On the atmospheric transmission of sun radiation and on dust in the air. Geogr. Ann. 11, 156–166.

Arhami, M., Kuhn, T., Fine, P.M., Delfino, R.J., Sioutas, C., 2006. Effects of Sampling Artifacts and Operating Parameters on the Performance of a Semicontinuous Particulate Elemental Carbon/Organic Carbon Monitor. Environ. Sci. Technol. 40, 945–954.

Arnott, W.P., Moosmüller, H., Rogers, C.F., Jin, T., Bruch, R., 1999. Photoacoustic spectrometer for measuring light absorption by aerosol: Instrument description. Atmos. Environ. 33, 2845–2852.

Artíñano, B., Salvador, P., Alonso, D.G., Querol, X., Alastuey, A., 2003. Anthropogenic and natural influence on the PM10 and PM2.5 aerosol in Madrid (Spain). Analysis of high concentration episodes. Environ. Pollut. 125, 453–465.

Bae, M.-S., Schauer, J.J., DeMinter, J.T., Turner, J.R., Smith, D., Cary, R.A., 2004. Validation of a semi-continuous instrument for elemental carbon and organic carbon using a thermal-optical method. Atmos. Environ. 38, 2885–2893.

Bauer, J.J., Yu, X.-Y., Cary, R., Laulainen, N., Berkowitz, C., 2009. Characterization of the Sunset Semi-Continuous Carbon Aerosol Analyzer. J. Air Waste Manage. Assoc. 59, 826–833.

Beeson, W.L., Abbey, D.E., Knutsen, S.F., 1998. Long-term concentrations of ambient air pollutants and

787 incident lung cancer in California adults: Results from the AHSMOG study. Environ. Health
788 Perspect. 106, 813–822.

789 Bergstrom, R.W., Pilewskie, P., Russell, P.B., Redemann, J., Bond, T.C., Quinn, P.K., Sierau, B., 2007.
790 Spectral absorption properties of atmospheric aerosols. Atmos. Chem. Phys. 7, 5937–5943.

791 Birch, M.E., Cary, R.A., 1996. Elemental carbon-based method for monitoring occupational exposures to
792 particulate diesel exhaust. Aerosol Sci. Technol. 25, 221–241.

793 Bond, T.C., Anderson, T.L., Campbell, D., 1999. Calibration and intercomparison of filter-based
794 measurements of visible light absorption by aerosols. Aerosol Sci. Technol. 30, 582–600.

795 Bond, T.C., Doherty, S.J., Fahey, D.W., Forster, P.M.D., Berntsen, T., DeAngelo, B.J., Flanner, M.G.,
796 Ghan, S., Kärcher, B., Koch, D., Kinne, S., Kondo, Y., Quinn, P.K., Sarofim, M.C., Schultz, M.G.,
797 Schulz, M., Venkataraman, C., Zhang, H., Zhang, S., Bellouin, N., Guttikunda, S.K., Hopke, P.K.,
798 Jacobson, M.Z., Kaiser, J.W., Klimont, Z., Lohmann, U., Schwarz, J.P., Shindell, D., Storelvmo, T.,
799 Warren, S.G., Zender, C.S., 2013. Bounding the role of black carbon in the climate system: A
800 scientific assessment. J. Geophys. Res. Atmos. 118, 5380–5552.

801 Cao, J., 2003. Characteristics of carbonaceous aerosol in Pearl River Delta Region, China during 2001
802 winter period. Atmos. Environ. 37, 1451–1460.

803 Caseiro, A., Bauer, H., Schmidl, C., Pio, C.A., Puxbaum, H., 2009. Wood burning impact on PM10 in
804 three Austrian regions. Atmos. Environ. 43, 2186–2195.

805 Castro, L.M., Pio, C.A., Harrison, R.M., Smith, D.J.T., 1999. Carbonaceous aerosol in urban and rural
806 European atmospheres: estimation of secondary organic carbon concentrations. Atmos. Environ. 33,
807 2771–2781.

808 Cavalli, F., Viana, M., Yttri, K.E., Genberg, J., Putaud, J.-P., 2010. Toward a standardised thermal-optical
809 protocol for measuring atmospheric organic and elemental carbon: the EUSAAR protocol. Atmos.
810 Meas. Tech. 3, 79–89.

811 Chylek, P., Coakley, J.A., 1974. Aerosols and Climate. Science. 183, 75–77.

812 Cong, Z., Kawamura, K., Kang, S., Fu, P., 2015. Penetration of biomass-burning emissions from South
813 Asia through the Himalayas: new insights from atmospheric organic acids. Sci. Rep. 5, 9580.

814 Crilley, L.R., Bloss, W.J., Yin, J., Beddows, D.C.S., Harrison, R.M., Allan, J.D., Young, D.E., Flynn, M.,
815 Williams, P., Zotter, P., Prevot, A.S.H., Heal, M.R., Barlow, J.F., Halios, C.H., Lee, J.D., Szidat, S.,
816 Mohr, C., 2015. Sources and contributions of wood smoke during winter in London: assessing local
817 and regional influences. Atmos. Chem. Phys. 15, 3149–3171.

818 Dockery, D.W., Pope, C.A., Xu, X., Spengler, J.D., Ware, J.H., Fay, M.E., Ferris, B.G.J., Speizer, F.E.,
819 1993. An Association between Air Pollution and Mortality in Six U.S. Cities. N. Engl. J. Med. 329,
820 1753–1759.

821 Drinovec, L., Močnik, G., Zotter, P., Prévôt, A.S.H., Ruckstuhl, C., Coz, E., Rupakheti, M., Sciare, J.,
822 Müller, T., Wiedensohler, A., Hansen, A.D.A., 2015. The “dual-spot” Aethalometer: an improved

measurement of aerosol black carbon with real-time loading compensation. Atmos. Meas. Tech. 8, 1965–1979.

Echalar, F., Gaudichet, A., Cachier, H., Artaxo, P., 1995. Aerosol emissions by tropical forest and savanna biomass burning: Characteristic trace elements and fluxes. Geophys. Res. Lett. 22, 3039–3042.

EEA, 1999. Criteria for EUROAIRNET. The EEA Air Quality Monitoring and Information Network. EEA Technical Report No 12.

Engling, G., Carrico, C.M., Kreidenweis, S.M., Collett Jr., J.L., Day, D.E., Malm, W.C., Lincoln, E., Min Hao, W., Iinuma, Y., Herrmann, H., 2006. Determination of levoglucosan in biomass combustion aerosol by high-performance anion-exchange chromatography with pulsed amperometric detection. Atmos. Environ. 40, 299–311.

Fabbri, D., Torri, C., Simoneit, B.R.T., Marynowski, L., Rushdi, A.I., Fabiańska, M.J., 2009. Levoglucosan and other cellulose and lignin markers in emissions from burning of Miocene lignites. Atmos. Environ. 43, 2286–2295.

Favez, O., Cachier, H., Sciare, J., Sarda-Estève, R., Martinon, L., 2009. Evidence for a significant contribution of wood burning aerosols to PM2.5 during the winter season in Paris, France. Atmos. Environ. 43, 3640–3644.

Favez, O., El Haddad, I., Piot, C., Boréave, A., Abidi, E., Marchand, N., Jaffrezo, J.-L.L., Besombes, J.-L.L., Personnaz, M.-B.B., Sciare, J., Wortham, H., George, C., D'Anna, B., 2010. Inter-comparison of source apportionment models for the estimation of wood burning aerosols during wintertime in an Alpine city (Grenoble, France). Atmos. Chem. Phys. 10, 5295–5314.

Fine, P.M., Cass, G.R., Simoneit, B.R.T., 2004. Chemical Characterization of Fine Particle Emissions from the Fireplace Combustion of Wood Types Grown in the Midwestern and Western United States. Environ. Eng. Sci. 21, 387–409.

Fourtziou, L., Liakakou, E., Stavroulas, I., Theodosi, C., Zarmpas, P., Psiloglou, B., Sciare, J., Maggos, T., Bairachtari, K., Bougiatioti, A., Gerasopoulos, E., Sarda-Estève, R., Bonnaire, N., Mihalopoulos, N., 2017. Multi-tracer approach to characterize domestic wood burning in Athens (Greece) during wintertime. Atmos. Environ. 148, 89–101.

Fuller, G.W., Tremper, A.H., Baker, T.D., Yttri, K.E., Butterfield, D., 2014. Contribution of wood burning to PM10 in London. Atmos. Environ. 87, 87–94.

Gao, S., Hegg, D.A., Hobbs, P. V., Kirchstetter, T.W., Magi, B.I., Sadilek, M., 2003. Water-soluble organic components in aerosols associated with savanna fires in southern Africa: Identification, evolution, and distribution. J. Geophys. Res. Atmos. 108.

GAW/WMO, 2012. "13th annual TFMM meeting, 17–19 April 2012, Gozo, Malta" (Position of the GAW Scientific Advisory Group on the use of Black Carbon terminology).

Gelencsér, A., 2004. Carbonaceous Aerosol, Atmospheric And Oceanographic Sciences Library. Springer

Netherlands, Dordrecht.

Gelencsér, A., May, B., Simpson, D., Sánchez-Ochoa, A., Kasper-Giebl, A., Puxbaum, H., Caseiro, A., Pio, C.A., Legrand, M., 2007. Source apportionment of PM2.5 organic aerosol over Europe: Primary/secondary, natural/anthropogenic, and fossil/biogenic origin. J. Geophys. Res. Atmos. 112, 1–12.

Gilardoni, S., Vignati, E., Cavalli, F., Putaud, J.P., Larsen, B.R., Karl, M., Stenström, K., Genberg, J., Henne, S., Dentener, F., 2011. Better constraints on sources of carbonaceous aerosols using a combined 14C – macro tracer analysis in a European rural background site. Atmos. Chem. Phys. 11, 5685–5700.

Graham, B., Mayol-Bracero, O.L., Guyon, P., Roberts, G.C., Decesari, S., Facchini, M.C., Artaxo, P., Maenhaut, W., Köll, P., Andreae, M.O., 2002. Water-soluble organic compounds in biomass burning aerosols over Amazonia1. Characterization by NMR and GC-MS. J. Geophys. Res. Atmos. 107, LBA 14-1--LBA 14-16.

Guha, A., Kumar De, B., Dhar, P., Banik, T., Chakraborty, M., Roy, R., Choudhury, A., Gogoi, M.M., Babu, S.S., Moorthy, K.K., 2015. Seasonal characteristics of aerosol black carbon in relation to long range transport over Tripura in Northeast India. Aerosol Air Qual. Res. 2015.

Hansen, A.D.A., Rosen, H., Novakov, T., 1984. The aethalometer — An instrument for the real-time measurement of optical absorption by aerosol particles. Sci. Total Environ. 36, 191–196.

Harrison, R.M., Beddows, D.C.S., Hu, L., Yin, J., 2012. Comparison of methods for evaluation of wood smoke and estimation of UK ambient concentrations. Atmos. Chem. Phys. 12, 8271–8283.

Harrison, R.M., Beddows, D.C.S.S., Jones, A.M., Calvo, A., Alves, C., Pio, C., 2013. An evaluation of some issues regarding the use of aethalometers to measure woodsmoke concentrations. Atmos. Environ. 80, 540–548.

Harrison, R.M., Yin, J., 2000. Particulate matter in the atmosphere: which particle properties are important for its effects on health? Sci. Total Environ. 249, 85–101.

Haywood, J.M., Boucher, O., 2000. Estimates of the direct and indirect radiative forcing due to tropospheric aerosols: A review. Rev. Geophys. 38, 513–543.

Heal, M.R., Hammonds, M.D., 2014. Insights into the composition and sources of rural, urban and roadside carbonaceous PM10. Environ. Sci. Technol. 48, 8995–9003.

Healy, R.M., Sciare, J., Poulain, L., Kamili, K., Merkel, M., Müller, T., Wiedensohler, A., Eckhardt, S., Stohl, A., Sarda-Estève, R., McGillicuddy, E., O'Connor, I.P., Sodeau, J.R., Wenger, J.C., 2012. Sources and mixing state of size-resolved elemental carbon particles in a European megacity: Paris. Atmos. Chem. Phys. 12, 1681–1700.

Herich, H., Gianini, M.F.D., Piot, C., Mo?nik, G., Jaffrezo, J.-L., Besombes, J.-L., Pr?v?t, A.S.H., Hueglin, C., 2014. Overview of the impact of wood burning emissions on carbonaceous aerosols and PM in large parts of the Alpine region. Atmos. Environ. 89, 64–75.

Herich, H., Hueglin, C., Buchmann, B., 2011. A 2.5 year's source apportionment study of black carbon from wood burning and fossil fuel combustion at urban and rural sites in Switzerland. Atmos. Meas. Tech. 4, 1409–1420.

Horvath, H., 1995. Estimation of the average visibility in central Europe. Atmos. Environ. 29, 241–246.

Huntzicker, J.J., Johnson, R.L., Shah, J.J., Cary, R.A., 1982. Analysis of Organic and Elemental Carbon in Ambient Aerosols by a Thermal-Optical Method, in: Particulate Carbon. Springer US, Boston, MA, pp. 79–88.

IPCC 2013, Stocker, T.F., Qin, D., Plattner, G.K., Tignor, M., Allen, S.K., Boschung, J., Nauels, A., Xia, Y., Bex, V., Midgley, P.M., IPCC 2013, Stocker, T.F., Qin, D., Plattner, G.K., Tignor, M., Allen, S.K., Boschung, J., Nauels, A., Xia, Y., Bex, V., Midgley, P.M., 2013. Climate Change 2013: The Physical Science Basis. Contribution of Working Group I to the Fifth Assessment Report of the Intergovernmental Panel on Climate Change.

Jamin, 1856. Neuer interferential-refractor. Ann. der Phys. und Chemie 174, 345–349.

Junta de Andalucía, 2016. Informe de Medio Ambiente en Andalucía 2015 (iMA).

Junta de Andalucía, 2015. Informe de Medio Ambiente en Andalucía 2014 (iMA).

Kirchstetter, T.W., Novakov, T., Hobbs, P. V., 2004. Evidence that the spectral dependence of light absorption by aerosols is affected by organic carbon. J. Geophys. Res. Atmos. 109, 1–12.

Krumal, K., Mikuska, P., Vecera, Z., 2012. Application of organic markers in identification of sources of organic aerosols. Chem. List. 106, 95–103.

Lim, S.S., Vos, T., Flaxman, A.D., Danaei, G., Shibuya, K., Adair-Rohani, H., AlMazroa, M.A., Amann, M., Anderson, H.R., Andrews, K.G., Aryee, M., Atkinson, C., Bacchus, L.J., Bahalim, A.N., Balakrishnan, K., Balmes, J., Barker-Collo, S., Baxter, A., Bell, M.L., Blore, J.D., Blyth, F., Bonner, C., Borges, G., Bourne, R., Boussinesq, M., Brauer, M., Brooks, P., Bruce, N.G., Brunekreef, B., Bryan-Hancock, C., Bucello, C., Buchbinder, R., Bull, F., Burnett, R.T., Byers, T.E., Calabria, B., Carapetis, J., Carnahan, E., Chafe, Z., Charlson, F., Chen, H., Chen, J.S., Cheng, A.T.-A., Child, J.C., Cohen, A., Colson, K.E., Cowie, B.C., Darby, S., Darling, S., Davis, A., Degenhardt, L., Dentener, F., Des Jarlais, D.C., Devries, K., Dherani, M., Ding, E.L., Dorsey, E.R., Driscoll, T., Edmond, K., Ali, S.E., Engell, R.E., Erwin, P.J., Fahimi, S., Falder, G., Farzadfar, F., Ferrari, A., Finucane, M.M., Flaxman, S., Fowkes, F.G.R., Freedman, G., Freeman, M.K., Gakidou, E., Ghosh, S., Giovannucci, E., Gmel, G., Graham, K., Grainger, R., Grant, B., Gunnell, D., Gutierrez, H.R., Hall, W., Hoek, H.W., Hogan, A., Hosgood, H.D., Hoy, D., Hu, H., Hubbell, B.J., Hutchings, S.J., Ibeanusi, S.E., Jacklyn, G.L., Jasrasaria, R., Jonas, J.B., Kan, H., Kanis, J.A., Kassebaum, N., Kawakami, N., Khang, Y.-H., Khatibzadeh, S., Khoo, J.-P., Kok, C., Laden, F., Lalloo, R., Lan, Q., Lathlean, T., Leasher, J.L., Leigh, J., Li, Y., Lin, J.K., Lipshultz, S.E., London, S., Lozano, R., Lu, Y., Mak, J., Malekzadeh, R., Mallinger, L., Marcenes, W., March, L., Marks, R., Martin, R., McGale, P., McGrath, J., Mehta, S., Memish, Z.A., Mensah, G.A., Merriman, T.R., Micha, R., Michaud, C., Mishra, V., Hanafiah, K.M., Mokdad, A.A., Morawska, L., Mozaffarian,

D., Murphy, T., Naghavi, M., Neal, B., Nelson, P.K., Nolla, J.M., Norman, R., Olives, C., Omer, S.B., Orchard, J., Osborne, R., Ostro, B., Page, A., Pandey, K.D., Parry, C.D., Passmore, E., Patra, J., Pearce, N., Pelizzari, P.M., Petzold, M., Phillips, M.R., Pope, D., Pope, C.A., Powles, J., Rao, M., Razavi, H., Rehfuess, E.A., Rehm, J.T., Ritz, B., Rivara, F.P., Roberts, T., Robinson, C., Rodriguez-Portales, J.A., Romieu, I., Room, R., Rosenfeld, L.C., Roy, A., Rushton, L., Salomon, J.A., Sampson, U., Sanchez-Riera, L., Sanman, E., Sapkota, A., Seedat, S., Shi, P., Shield, K., Shivakoti, R., Singh, G.M., Sleet, D.A., Smith, E., Smith, K.R., Stapelberg, N.J., Steenland, K., Stöckl, H., Stovner, L.J., Straif, K., Straney, L., Thurston, G.D., Tran, J.H., Van Dingenen, R., van Donkelaar, A., Veerman, J.L., Vijayakumar, L., Weintraub, R., Weissman, M.M., White, R.A., Whiteford, H., Wiersma, S.T., Wilkinson, J.D., Williams, H.C., Williams, W., Wilson, N., Woolf, A.D., Yip, P., Zielinski, J.M., Lopez, A.D., Murray, C.J., Ezzati, M., 2012. A comparative risk assessment of burden of disease and injury attributable to 67 risk factors and risk factor clusters in 21 regions, 1990–2010: a systematic analysis for the Global Burden of Disease Study 2010. Lancet 380, 2224–2260.

Lohmann, U., Feichter, J., 2005. Global indirect aerosol effects: a review. Atmos. Chem. Phys. 5, 715–737.

Madrid City Council, 2016. Madrid 2015 Annual air quality assessment report (Calidad del aire Madrid 2015). General Directorate of Sustainability and Environmental Control, Madrid City Council.

Madrid City Council, 2015. Inventario de emisiones de contaminantes a la atmósfera en el municipio de Madrid 2013.

MAPAMA Ministry of Agriculture and Fisheries Food and Environment, 2017. Evaluación de la calidad del aire en España 2015.

Martinsson, J., Abdul Azeem, H., Sporre, M.K., Bergström, R., Ahlberg, E., Öström, E., Kristensson, A., Swietlicki, E., Eriksson Stenström, K., 2017. Carbonaceous aerosol source apportionment using the Aethalometer model – evaluation by radiocarbon and levoglucosan analysis at a rural background site in southern Sweden. Atmos. Chem. Phys. 17, 4265–4281.

Miyazaki, Y., Kondo, Y., Sahu, L.K., Imaru, J., Fukushima, N., Kano, M., 2008. Performance of a newly designed continuous soot monitoring system (COSMOS). J. Environ. Monit. 10, 1195–1201.

Mohr, C., Richter, R., DeCarlo, P.F., Prévôt, A.S.H., Baltensperger, U., 2011. Spatial variation of chemical composition and sources of submicron aerosol in Zurich during wintertime using mobile aerosol mass spectrometer data. Atmos. Chem. Phys. 11, 7465–7482.

Moorthy, K.K., Nair, V.S., Babu, S.S., Satheesh, S.K., 2009. Spatial and vertical heterogeneities in aerosol properties over oceanic regions around India: Implications for radiative forcing. Q. J. R. Meteorol. Soc. 135, 2131–2145.

Moosmüller, H., Chakrabarty, R.K., Ehlers, K.M., Arnott, W.P., 2011. Absorption Ångström coefficient, brown carbon, and aerosols: basic concepts, bulk matter, and spherical particles. Atmos. Chem. Phys. 11, 1217–1225.

969 Moreno, T., Querol, X., Castillo, S., Alastuey, A., Cuevas, E., Herrmann, L., Mounkaila, M., Elvira, J.,
970 Gibbons, W., 2006. Geochemical variations in aeolian mineral particles from the Sahara–Sahel
971 Dust Corridor. Chemosphere 65, 261–270.

972 Na, K., Sawant, A.A., Song, C., Cocker, D.R., 2004. Primary and secondary carbonaceous species in the
973 atmosphere of Western Riverside County, California. Atmos. Environ. 38, 1345–1355.

974 Nolte, C.G., Schauer, J.J., Cass, G.R., Simoneit, B.R.T., 2001. Highly polar organic compounds present
975 in wood smoke and in the ambient atmosphere. Environ. Sci. Technol. 35, 1912–1919.

976 Oanh, N.T.K., Ly, B.T., Tipayarom, D., Manandhar, B.R., Prapat, P., Simpson, C.D., Sally Liu, L.-J.,
977 2011. Characterization of particulate matter emission from open burning of rice straw. Atmos.
978 Environ. 45, 493–502.

979 Penner, J.E., Novakov, T., 1996. Carbonaceous particles in the atmosphere: A historical perspective to the
980 Fifth International Conference on Carbonaceous Particles in the Atmosphere. J. Geophys. Res.
981 Atmos. 101, 19373–19378.

982 Petit, J.-E., Favez, O., Sciare, J., Canonaco, F., Croteau, P., Močnik, G., Jayne, J., Worsnop, D., Leoz-
983 Garziandia, E., 2014. Submicron aerosol source apportionment of wintertime pollution in Paris,
984 France by double positive matrix factorization (PMF2) using an aerosol chemical speciation
985 monitor (ACSM) and a multi-wavelength Aethalometer. Atmos. Chem. Phys. 14, 13773–13787.

986 Petit, J.-E., Favez, O., Sciare, J., Crenn, V., Sarda-Estève, R., Bonnaire, N., Močnik, G., Dupont, J.-C.,
987 Haeffelin, M., Leoz-Garziandia, E., 2015. Two years of near real-time chemical composition of
988 submicron aerosols in the region of Paris using an Aerosol Chemical Speciation Monitor (ACSM)
989 and a multi-wavelength Aethalometer. Atmos. Chem. Phys. 15, 2985–3005.

990 Petzold, A., Ogren, J.A., Fiebig, M., Laj, P., Li, S.-M., Baltensperger, U., Holzer-Popp, T., Kinne, S.,
991 Pappalardo, G., Sugimoto, N., Wehrli, C., Wiedensohler, A., Zhang, X.-Y., 2013.
992 Recommendations for reporting “black carbon” measurements. Atmos. Chem. Phys. 13, 8365–
993 8379.

994 Petzold, A., Schönlinner, M., 2004. Multi-angle absorption photometry - A new method for the
995 measurement of aerosol light absorption and atmospheric black carbon. J. Aerosol Sci. 35, 421–
996 441.

997 Piazzola, J., Sellegri, K., Bourcier, L., Mallet, M., Tedeschi, G., Missamou, T., 2012. Physicochemical
998 characteristics of aerosols measured in the spring time in the Mediterranean coastal zone. Atmos.
999 Environ. 54, 545–556.

1000 Pio, C.A., Legrand, M., Alves, C.A., Oliveira, T., Afonso, J., Caseiro, A., Puxbaum, H., Sanchez-Ochoa,
1001 A., Gelencsér, A., 2008. Chemical composition of atmospheric aerosols during the 2003 summer
1002 intense forest fire period. Atmos. Environ. 42, 7530–7543.

1003 Pio, C.A., Legrand, M., Oliveira, T., Afonso, J., Santos, C., Caseiro, A., Fialho, P., Barata, F., Puxbaum,
1004 H., Sanchez-Ochoa, A., Kasper-Giebl, A., Gelencsér, A., Preunkert, S., Schock, M., 2007.
1005 Climatology of aerosol composition (organic versus inorganic) at nonurban sites on a west-east

transect across Europe. J. Geophys. Res. 112, D23S02.

Pio, C., Castro, L.M., Ramos, M.O., 1994. Differentiated determination of organic and elemental carbon in atmospheric aerosol particles by a thermal–optical method, in: Angeletti, G., Restelli, G. (Eds.), Proceedings of the Sixth European Symposium on Physico-Chemical Behavior of Atmospheric Pollutants. pp. 706–711.

Pio, C., Cerqueira, M., Harrison, R.M., Nunes, T., Mirante, F., Alves, C., Oliveira, C., Sanchez de la Campa, A., Artíñano, B., Matos, M., 2011. OC/EC ratio observations in Europe: Re-thinking the approach for apportionment between primary and secondary organic carbon. Atmos. Environ. 45, 6121–6132.

Plaza, J., Artíñano, B., Salvador, P., Gómez-Moreno, F.J., Pujadas, M., Pio, C.A., 2011. Short-term secondary organic carbon estimations with a modified OC/EC primary ratio method at a suburban site in Madrid (Spain). Atmos. Environ. 45, 2496–2506.

Pope, C.A., Burnett, R.T., Thun, M.J., Calle, E.E., Krewski, D., Ito, K., Thurston, G.D., 2002. Lung Cancer, Cardiopulmonary Mortality, and Long-term Exposure to Fine Particulate Air Pollution. JAMA J. Am. Med. Assoc. 287, 1132–1141.

Putaud, J.-P., Van Dingenen, R., Alastuey, A., Bauer, H., Birmili, W., Cyrys, J., Flentje, H., Fuzzi, S., Gehrig, R., Hansson, H.C., Harrison, R.M., Herrmann, H., Hitzenberger, R., Hüglin, C., Jones, A.M., Kasper-Giebl, A., Kiss, G., Kousa, A., Kuhlbusch, T.A.J., Löschau, G., Maenhaut, W., Molnar, A., Moreno, T., Pekkanen, J., Perrino, C., Pitz, M., Puxbaum, H., Querol, X., Rodriguez, S., Salma, I., Schwarz, J., Smolik, J., Schneider, J., Spindler, G., ten Brink, H., Tursic, J., Viana, M., Wiedensohler, A., Raes, F., 2010. A European aerosol phenomenology – 3: Physical and chemical characteristics of particulate matter from 60 rural, urban, and kerbside sites across Europe. Atmos. Environ. 44, 1308–1320.

Putaud, J.-P.P., Raes, F., Van Dingenen, R., Brüggemann, E., Facchini, M.C., Decesari, S., Fuzzi, S., Gehrig, R., Hüglin, C., Laj, P., Lorbeer, G., Maenhaut, W., Mihalopoulos, N., Müller, K., Querol, X., Rodriguez, S., Schneider, J., Spindler, G., Brink, H. ten, Tørseth, K., Wiedensohler, A., 2004. A European aerosol phenomenology—2: chemical characteristics of particulate matter at kerbside, urban, rural and background sites in Europe. Atmos. Environ. 38, 2561–2577.

Puxbaum, H., Caseiro, A., Sánchez-Ochoa, A., Kasper-Giebl, A., Claeys, M., Gelencsér, A., Legrand, M., Preunkert, S., Pio, C., 2007. Levoglucosan levels at background sites in Europe for assessing the impact of biomass combustion on the European aerosol background. J. Geophys. Res. 112, D23S05.

Querol, X., Alastuey, A., Rodríguez, S., Viana, M.M., Artíñano, B., Salvador, P., Mantilla, E., do Santos, S.G., Patier, R.F., de La Rosa, J., de la Campa, A.S., Menéndez, M., Gil, J.J., 2004a. Levels of particulate matter in rural, urban and industrial sites in Spain. Sci. Total Environ. 334–335, 359–376.

Querol, X., Alastuey, A., Ruiz, C.R., Artiñano, B., Hansson, H.C., Harrison, R.M., Buringh, E., Ten

1043 Brink, H.M., Lutz, M., Bruckmann, P., Straehl, P., Schneider, J., 2004b. Speciation and origin of
1044 PM10 and PM2.5 in selected European cities. Atmos. Environ. 38, 6547–6555.

1045 Querol, X., Alastuey, A., Viana, M., Moreno, T., Reche, C., Minguillón, M.C., Ripoll, A., Pandolfi, M.,
1046 Amato, F., Karanasiou, A., Pérez, N., Pey, J., Cusack, M., Vázquez, R., Plana, F., Dall'Osto, M., de
1047 la Rosa, J., Sánchez de la Campa, A., Fernández-Camacho, R., Rodríguez, S., Pio, C., Alados-
1048 Arboledas, L., Titos, G., Artíñano, B., Salvador, P., García Dos Santos, S., Fernández Patier, R.,
1049 2013. Variability of carbonaceous aerosols in remote, rural, urban and industrial environments in
1050 Spain: implications for air quality policy. Atmos. Chem. Phys. 13, 6185–6206.

1051 Ram, K., Sarin, M.M., 2010. Spatio-temporal variability in atmospheric abundances of EC, OC and
1052 WSOC over Northern India. J. Aerosol Sci., International geophysics series 41, 88–98.

1053 Reche, C., Querol, X., Alastuey, A., Viana, M., Pey, J., Moreno, T., Rodríguez, S., González, Y.,
1054 Fernández-Camacho, R., de la Rosa, J., Dall'Osto, M., Prévôt, A.S.H., Hueglin, C., Harrison, R.M.,
1055 Quincey, P., 2011. New considerations for PM, Black Carbon and particle number concentration for
1056 air quality monitoring across different European cities. Atmos. Chem. Phys. 11, 6207–6227.

1057 Russell, P.B., Bergstrom, R.W., Shinozuka, Y., Clarke, A.D., DeCarlo, P.F., Jimenez, J.L., Livingston,
1058 J.M., Redemann, J., Dubovik, O., Strawa, A., 2010. Absorption Angstrom Exponent in AERONET
1059 and related data as an indicator of aerosol composition. Atmos. Chem. Phys. 10, 1155–1169.

1060 Salvador, P., Artíñano, B., Becerril, M., Coz, E., García-Alonso, S., Pérez-Pastor, R., 2016.
1061 Caracterización de material particulado atmosférico en Villanueva del Arzobispo (Jaén): niveles,
1062 composición química y origen (No. INF-METALAB-2016-03).

1063 Salvador, P., Artíñano, B., G. Alonso, D., Querol, X., Alastuey, A., 2004. Identification and
1064 characterisation of sources of PM10 in Madrid (Spain) by statistical methods. Atmos. Environ. 38,
1065 435–447.

1066 Salvador, P., Artíñano, B., Viana, M., Alastuey, A., Querol, X., 2012. Evaluation of the changes in the
1067 Madrid metropolitan area influencing air quality: Analysis of 1999–2008 temporal trend of
1068 particulate matter. Atmos. Environ. 57, 175–185.

1069 Salvador, P., Artíñano, B., Viana, M.M., Alastuey, A., Querol, X., 2015. Multicriteria approach to
1070 interpret the variability of the levels of particulate matter and gaseous pollutants in the Madrid
1071 metropolitan area, during the 1999–2012 period. Atmos. Environ. 109, 205–216.

1072 Sánchez de la Campa, A.M., Pio, C., de la Rosa, J., Querol, X., Alastuey, A., González-Castanedo, Y.,
1073 2009. Characterization and origin of EC and OC particulate matter near the Doñana National Park
1074 (SW Spain). Environ. Res. 109, 671–681.

1075 Sandradewi, J., Prévôt, A.S.H., Szidat, S., Perron, N., Alfarra, M.R., Lanz, V.A., Weingartner, E.,
1076 Baltensperger, U., 2008a. Using Aerosol Light Absorption Measurements for the Quantitative
1077 Determination of Wood Burning and Traffic Emission Contributions to Particulate Matter. Environ.
1078 Sci. Technol. 42, 3316–3323.

1079 Sandradewi, J., Prévôt, A.S.H., Weingartner, E., Schmidhauser, R., Gysel, M., Baltensperger, U., 2008b.

A study of wood burning and traffic aerosols in an Alpine valley using a multi-wavelength Aethalometer. Atmos. Environ. 42, 101–112.

Sandrini, S., Fuzzi, S., Piazzalunga, A., Prati, P., Bonasoni, P., Cavalli, F., Bove, M.C., Calvello, M., Cappelletti, D., Colombi, C., Contini, D., de Gennaro, G., Di Gilio, A., Fermo, P., Ferrero, L., Gianelle, V., Giugliano, M., Ielpo, P., Lonati, G., Marinoni, A., Massabò, D., Molteni, U., Moroni, B., Pavese, G., Perrino, C., Perrone, M.G., Perrone, M.R., Putaud, J.-P., Sargolini, T., Vecchi, R., Gilardoni, S., 2014. Spatial and seasonal variability of carbonaceous aerosol across Italy. Atmos. Environ. 99, 587–598.

Satheesh, S., Krishnamoorthy, K., 2005. Radiative effects of natural aerosols: A review. Atmos. Environ. 39, 2089–2110.

Schauer, J.J., Cass, G.R., 2000. Source Apportionment of Wintertime Gas-Phase and Particle-Phase Air Pollutants Using Organic Compounds as Tracers. Environ. Sci. Technol. 34, 1821–1832.

Schmidl, C., Marr, I.L., Caseiro, A., Kotianová, P., Berner, A., Bauer, H., Kasper-Giebl, A., Puxbaum, H., 2008. Chemical characterisation of fine particle emissions from wood stove combustion of common woods growing in mid-European Alpine regions. Atmos. Environ. 42, 126–141.

Schwarz, J., Cusack, M., Karban, J., Chalupníčková, E., Havránek, V., Smolík, J., Ždímal, V., 2016. PM2.5 chemical composition at a rural background site in Central Europe, including correlation and air mass back trajectory analysis. Atmos. Res. 176–177, 108–120.

Seinfeld, J.H., Pandis, S.N., 2006. Atmospheric Chemistry and Physics: From Air Pollution to Climate Change, 2nd Edition.

Seinfeld, J.H., Pankow, J.F., 2003. Organic atmospheric particulate material. Annu. Rev. Phys. Chem. 54, 121–140.

Shine, K.P., Forster, P.M.D., 1999. The effect of human activity on radiative forcing of climate change: a review of recent developments. Glob. Planet. Change 20, 205–225.

Sigsgaard, T., Forsberg, B., Annesi-Maesano, I., Blomberg, A., Bølling, A., Boman, C., Bønløkke, J., Brauer, M., Bruce, N., Héroux, M.-E., Hirvonen, M.-R., Kelly, F., Künzli, N., Lundbäck, B., Moshammer, H., Noonan, C., Pagels, J., Sallsten, G., Sculier, J.-P., Brunekreef, B., 2015. Health impacts of anthropogenic biomass burning in the developed world. Eur. Respir. J. 46, 1577–1588.

Simoneit, B.R.T., 2002. Biomass burning — a review of organic tracers for smoke from incomplete combustion. Appl. Geochemistry 17, 129–162.

Simoneit, B.R.T., Schauer, J.J., Nolte, C.G., Oros, D.R., Elias, V.O., Fraser, M.P., Rogge, W.F., Cass, G.R., 1999. Levoglucosan, a tracer for cellulose in biomass burning and atmospheric particles. Atmos. Environ. 33, 173–182.

Titos, G., del Águila, A., Cazorla, A., Lyamani, H., Casquero-Vera, J.A., Colombi, C., Cuccia, E., Gianelle, V., Močnik, G., Alastuey, A., Olmo, F.J., Alados-Arboledas, L., 2017. Spatial and temporal variability of carbonaceous aerosols: Assessing the impact of biomass burning in the

1116 urban environment. Sci. Total Environ. 578, 613–625.

1117 Titos, G., Lyamani, H., Drinovec, L., Olmo, F.J., Močnik, G., Alados-Arboledas, L., 2015. Evaluation of
1118 the impact of transportation changes on air quality. Atmos. Environ. 114, 19–31.

1119 Twomey, S., 1974. Pollution and the planetary albedo. Atmos. Environ. 8, 1251–1256.

1120 UNE-EN 12341:1999, n.d. Air quality: Determination of the PM10 fraction of the suspended particulate
1121 matter. Reference method and field test procedure to demonstrate reference equivalence of
1122 measurement methods.

1123 UNE-EN 14907:2006, n.d. Ambient air quality: Standard gravimetric measurement method for the
1124 determination of the PM2.5 mass fraction of suspended particulate matter.

1125 UNEP-CCAC, 2014. Time to act to reduce short-lived climate pollutants.

1126 UNEP, WMO, 2011. Integrated Assessment of Black Carbon and Tropospheric Ozone. Environment 30.

1127 US EPA, 2012. Report to Congress on Black Carbon.

1128 Viana, M., Kuhlbusch, T.A.J., Querol, X., Alastuey, A., Harrison, R.M., Hopke, P.K., Winiwarter, W.,
1129 Vallius, M., Szidat, S., Prévôt, A.S.H., Hueglin, C., Bloemen, H., Wåhlin, P., Vecchi, R., Miranda,
1130 A.I., Kasper-Giebl, A., Maenhaut, W., Hitzenberger, R., 2008. Source apportionment of particulate
1131 matter in Europe: A review of methods and results. J. Aerosol Sci. 39, 827–849.

1132 Wang, J., Christopher, S.A., 2003. Intercomparison between satellite-derived aerosol optical thickness
1133 and PM 2.5 mass: Implications for air quality studies. Geophys. Res. Lett. 30, 2–5.

1134 WHO, 2012. Health effects of black carbon. World Heal. Organ.

1135 Zanatta, M., Gysel, M., Bukowiecki, N., Müller, T., Weingartner, E., Areskoug, H., Fiebig, M., Yttri,
1136 K.E., Mihalopoulos, N., Kouvarakis, G., Beddows, D., Harrison, R.M., Cavalli, F., Putaud, J.P.,
1137 Spindler, G., Wiedensohler, A., Alastuey, A., Pandolfi, M., Sellegri, K., Swietlicki, E., Jaffrezo,
1138 J.L., Baltensperger, U., Laj, P., 2016. A European aerosol phenomenology-5: Climatology of black
1139 carbon optical properties at 9 regional background sites across Europe. Atmos. Environ. 145, 346–
1140 364.

1141 Zhang, Y., Shao, M., Zhang, Y., Zeng, L., He, L., Zhu, B., Wei, Y., Zhu, X., 2007. Source profiles of
1142 particulate organic matters emitted from cereal straw burnings. J. Environ. Sci. 19, 167–175.

1143 Zhu, J., Crozier, P.A., Aoki, T., Anderson, J.R., 2014. Full Optical Properties of Carbonaceous Aerosols
1144 by High Energy Monochromated Electron Energy-loss Spectroscopy. Microsc. Microanal. 20, 188–
1145 189.

1146 Zotter, P., Herich, H., Gysel, M., El-Haddad, I., Zhang, Y., Močnik, G., Hüglin, C., Baltensperger, U.,
1147 Szidat, S., Prévôt, A.S.H., 2017. Evaluation of the absorption Ångström exponents for traffic and
1148 wood burning in the Aethalometer-based source apportionment using radiocarbon measurements of
1149 ambient aerosol. Atmos. Chem. Phys. 17, 4229–4249.

1150

HIGHLIGHTS

- One-year black carbon (BC) experimental study at three different locations in Spain.
- Estimation of fossil fuel and biomass burning absorption Ångström exponents.
- Source apportionment of black carbon from fossil fuel and biomass burning.
- Dominance of fossil fuel at urban sites and biomass burning in winter at rural area.
- Relationship between BC with biomass burning tracers, organic and elemental carbon.